

Dynamic Weights in Gaussian Mixture Models: A Bayesian Approach

Michel H. Montoril*

Department of Statistics, Federal University of São Carlos, Brazil

and

Leandro T. Correia

Department of Statistics, University of Brasília, Brazil

and

Helio S. Migon†

Federal University of Rio Janeiro, Brazil

November 18, 2021

Abstract

In this paper we consider a Gaussian mixture model where the mixture weight behaves as an unknown function of time. To estimate the mixture weight function, we develop a Bayesian nonlinear dynamic approach for polynomial models. Two estimation methods that can be extended to other situations are considered. One of them, called here component-wise Metropolis-Hastings, is more general and can be used for any situation where the observation and state equations are nonlinearly connected. The other method tends to be faster but must be applied specifically to binary data (by using a probit link function). This kind of Gaussian mixture model is capable of successfully capturing the features of the data, as observed in numerical studies. It can be useful in studies such as clustering, change-point and process control. We apply the proposed method an array Comparative Genomic Hybridization (aCGH) dataset from glioblastoma cancer studies, where we illustrate the ability of the new method to detect chromosome aberrations.

Keywords: change-point, classification, cluster, dynamic models, mixture problem, regime switching, state-space models

*corresponding author: michel@ufscar.br

†Visiting professor at IMECC / Unicamp

1 Introduction

Gaussian mixture models (GMM) have been used to solve problems in a wide range of fields, under different scenarios. In the context of statistical learning, these models play an important role. We can highlight clustering (Saraiva and Milan, 2012) and classification (Fernando et al., 2012) as unsupervised and supervised learning examples. For more details and examples, see Hastie et al. (2017).

This important role played by GMMs makes them topics of interest of various researchers, who have improved and generalized this class in the context of (homogeneous) hidden Markov models (HMM). Examples range from econometrics (Tobias Rydén et al., 1998) to genetics (Boys and Henderson, 2004). Also, Robert et al. (2000) made use of reversible jump Markov chain Monte Carlo (RJ-MCMC) to estimate parameters in this class of models. In the multivariate case, Spezia (2010) introduced Gaussian hidden Markov models with unknown number of regimes. An interesting reference with wide applicability of GMMs is the book by Bouguila and Fan (2020).

Still in terms of generalization, we can mention the non-homogeneous HMM (NH-HMM), where the transition probabilities are not constant. For example, Raymond and Rich (1997) considered binary probit models to link covariates to the transition probabilities; Meligkotsidou and Dellaportas (2011) developed a Bayesian forecasting method where the transition probabilities depend on covariates; Holsclaw et al. (2017) developed an efficient MCMC sampling scheme by extending the Pólya-Gamma data augmentation to handle NH-HMMs; and Spezia (2020) proposed an evolutionary Monte Carlo algorithm based on a Bayesian method for stochastic selection of covariates to explain the variation of the transition probabilities.

In this work we consider a type of non-homogeneous HMM. To be more specific, we analyze a typical GMM, but use a state-space (SS) approach to model the time evolution of the mixture

weights. Both classes, SS and HMM, are similar in the sense that they relate unobserved states to responses. In SS, the states are continuous, while in HMM they are discrete (Fahrmeir and Tutz, 2001). This makes the model flexible and better able to capture the data features. The model allows for classification, clustering, change-points and process control. A similar model was studied by Montoril et al. (2019), where the authors considered the mixture of two random variables (r.v.'s) with known means and variances, but with unknown time-varying mixture weights (estimated by wavelet bases). On the other hand, in this paper we deal with unknown means and variances for the mixture components. Furthermore, we consider Bayesian nonlinear dynamic models to estimate the mixture weights. These models have the dynamic generalized linear model studied by West et al. (1985) as special case. A variant of the simple and efficient MCMC algorithm for SS by Chan and Jeliazkov (2009) is proposed. A simple reformulation of the SS, exploring the nature of the dynamic polynomial models, leads to an efficient simulation algorithm that is scalable and widely applicable.

This paper is organized as follows. In Section 2, the Gaussian mixture model is introduced and its inference is discussed. In Section 3, a proposed Bayesian model for nonlinear dynamic models is discussed. This method is employed for estimation of the dynamic mixture weights. The performance of the proposed method is evaluated in Section 4 by using simulated datasets, where four different functional behaviors are studied. We approach two main cases: dynamic binomial data and Gaussian mixture data. In Section 5, we apply the method to an array Comparative Genomic Hybridization (aCGH) dataset from glioblastoma cancer studies. Some concluding remarks are given in Section 6.

2 The Gaussian mixture model

In this paper, we examine a dynamic Bayesian mixture of independent Gaussian distributions, with unknown means and precisions. The model can be specified as

$$y_t|z_t, \boldsymbol{\mu}, \boldsymbol{\phi} \sim N[z_t'\boldsymbol{\mu}, (z_t'\boldsymbol{\phi})^{-1}], \quad (1)$$

$$z_t|\boldsymbol{\alpha}_t \sim \text{Cat}(\boldsymbol{\alpha}_t),$$

$t = 1, \dots, T$, where the y_t 's are observed components, and the z_t 's are latent components, that indicate the normal population to which the t -th observation belongs. In other words, $z_t = (z_{1t}, \dots, z_{Kt})'$ is a vector such that $z_{kt} = 1$, if y_t belongs to the k -th normal population, and zero otherwise. Moreover, $\boldsymbol{\mu} = (\mu_1, \dots, \mu_K)'$ and $\boldsymbol{\phi} = (\phi_1, \dots, \phi_K)'$ represent the mean and precision vectors, respectively. Also, $\text{Cat}(\cdot)$ can be used to denote a categorical variable, and $\boldsymbol{\alpha}_t = (\alpha_{1t}, \dots, \alpha_{Kt})'$ corresponds to the mixture weights at time t , with $\alpha_{kt} \geq 0$ and $\sum_{k=1}^K \alpha_{kt} = 1$. Each weight α_{kt} characterizes the probability that $z_{kt} = 1$.

The main goal in this section is the estimation of $\boldsymbol{\mu}$, $\boldsymbol{\phi}$ and the z_t 's. In order to derive the posterior distribution of these parameters, we assume that $p(\mathbf{y}|\mathbf{z}, \boldsymbol{\mu}, \boldsymbol{\phi}) = \prod_{t=1}^T p(y_t|z_t, \boldsymbol{\mu}, \boldsymbol{\phi})$ and $p(\mathbf{z}|\boldsymbol{\alpha}_1, \dots, \boldsymbol{\alpha}_T) = \prod_{t=1}^T p(z_t|\boldsymbol{\alpha}_t)$. This means that y_t is a time series and its dependence structure is mostly related to the functional behavior of the probability of mixture sequence $\boldsymbol{\alpha}_t$.

The case where $\boldsymbol{\alpha}_t \equiv \boldsymbol{\alpha}$ corresponds to the ordinary Gaussian mixture model, and it is taken into account in this section (which does not interfere in the results for the component parameters). There is a vast literature for this setup. A comprehensive survey involving finite mixture models, under several scenarios, is presented in Frühwirth-Schnatter (2006).

It is a usual practice to postulate independent prior distributions for the component parameters $\boldsymbol{\mu}$ and $\boldsymbol{\phi}$, i.e., $p(\boldsymbol{\mu}, \boldsymbol{\phi}) = \prod_{k=1}^K p(\mu_k)p(\phi_k)$. Examples of works employing independent priors are Escobar and West (1995) and Richardson and Green (1997). We consider in this paper $\mu_k \sim$

$N(\mu_{0k}, \sigma_{0k}^2)$ and $\phi_k \sim \Gamma(\nu_{0k}, \eta_{0k})$, $k = 1, \dots, K$. When $\alpha_t \equiv \alpha$, the prior of the mixture weights vector α is usually a Dirichlet process, $\alpha \sim Dir(\mathbf{e}_0)$, which is assumed to be independent of $\boldsymbol{\mu}$ and $\boldsymbol{\phi}$.

2.1 Full conditional posterior distributions of the component parameters

In order to get the full conditional distributions, we begin by specifying the joint distribution of the observations, latent quantities and parameters:

$$p(\mathbf{y}, \mathbf{z}, \boldsymbol{\mu}, \boldsymbol{\phi}, \boldsymbol{\alpha}) = p(\mathbf{y}|\boldsymbol{\mu}, \boldsymbol{\phi}, \mathbf{z})p(\boldsymbol{\mu}, \boldsymbol{\phi})p(\mathbf{z}|\boldsymbol{\alpha})p(\boldsymbol{\alpha}).$$

We denote by $[\dots]$ the set of all remaining variables to be considered for the posterior in use.

It is straightforward to obtain that:

- (i) the conditional posterior distribution for each mean and precision value are, respectively,

$$\mu_k | \mathbf{y}, [\dots] \sim N(\bar{\mu}_k, \bar{\sigma}_k^2), \quad (2)$$

$$\phi_k | \mathbf{y}, [\dots] \sim \Gamma(\bar{\nu}_k, \bar{\eta}_k), \quad (3)$$

where

$$\begin{aligned} \bar{\sigma}_k^2 &= (T_k \phi_k + 1/\sigma_{0k}^2)^{-1}, & \bar{\nu}_k &= \nu_{0k} + T_k/2, \\ \bar{\mu}_k &= \bar{\sigma}_k^2 (s_k \phi_k + \mu_{0k}/\sigma_{0k}^2), & \bar{\eta}_k &= \eta_{0k} + v_k, \end{aligned}$$

with $T_k = \#\{z_{kt} = 1, t = 1, \dots, T\}$, $s_k = \sum_{\{t: z_{kt}=1\}} y_t$ and $v_k = \sum_{\{t: z_{kt}=1\}} (y_t - \mu_k)^2$, $k = 1, \dots, K$;

- (ii) the conditional posterior distribution of the latent categorical variable is $p(z_{kt} = 1 | \mathbf{y}, [\dots]) \propto \alpha_k \varphi(y_t | \mu_k, \phi_k^{-1})$, where $\varphi(x|a, b)$ denotes the probability density function of a normal r.v. with mean a and variance b . Then, it follows that

$$P(z_{kt} = 1 | \mathbf{y}, [\dots]) = \frac{\alpha_k \varphi(y_t | \mu_k, \phi_k^{-1})}{\sum_{k=1}^K \alpha_k \varphi(y_t | \mu_k, \phi_k^{-1})}, \quad k = 1, \dots, K;$$

(iii) for the sake of information, the conditional posterior of the mixture weights is

$$\boldsymbol{\alpha}|\mathbf{y}, [\dots] \sim \text{Dir}(\mathbf{e}_1), \text{ where } \mathbf{e}_1 = \mathbf{e}_0 + (T_1, \dots, T_K)'$$

A frequent issue involving mixture problems is label switching. There are several studies suggesting solutions to this kind of problem (more details in Frühwirth-Schnatter, 2006). Here, we consider a simple solution: the pairs (μ_k, ϕ_k) are ordered under the constraint $\mu_k < \mu_{k+1}$.

As mentioned before, the full conditional posteriors in the case where the weights are dynamic are the same as in (i) and (ii) above. Thus, it remains to study situations where the mixture weights vary over time.

3 The dynamic mixture weights

For the sake of simplicity, we consider the case where $K = 2$, i.e., a dynamic Gaussian mixture of two groups. In this scenario, z_t is equivalent to a Bernoulli r.v. with parameter α_t , the dynamic mixture weight. Therefore, we focus on the general case where α_t varies throughout time. In this section, we begin with a short review of polynomial dynamic models. Next we discuss the inference for this class of models, following an alternative route than the usual FFBS (Frühwirth-Schnatter, 1994), based on Chan and Jeliazkov (2009). The polynomial model structure is explored to make some improvements in the Chan's algorithm in the Gaussian scenario. Then a generalization to the nonlinear situation is explored, which includes the estimation of the α_t 's.

3.1 Univariate DLM and polynomial models

Following West and Harrison (1997), we define a dynamic linear model (DLM) by the quadruple $\{\mathbf{F}, \mathbf{G}, V, \mathbf{W}\}_t$, where \mathbf{F}_t is a known vector of constants or predictor variables (features or regressors), \mathbf{G}_t is a known state vector ($\boldsymbol{\theta}_t$) evolution matrix, \mathbf{W}_t is the variance of the stochastic

evolution innovation vector, and V_t is the observational variance. Without loss of generality, we assume that $\mathbf{W}_t = \text{diag}\{W_1, \dots, W_p\}$, $\forall t$. A very useful subclass of dynamic models is the time series dynamic model (TSDLM), characterized by $\mathbf{F}_t = \mathbf{F}$, $\forall t$ and $\mathbf{G}_t = \mathbf{I}$, $\forall t$, where \mathbf{I} is an identity matrix. In this paper, we devote special attention to the polynomial DLM. Any observable TSDLM that, for all $t \geq 0$, has a forecast function in the form $f_t(k) = a_{t,0} + a_{t,1}k + \dots + a_{t,p-1}k^{p-1}$, $k > 0$, is defined as the p -th order polynomial DLM. The p -th order polynomial model is similar to the canonical model: $\mathbf{F}_t = (1, 0, \dots, 0)'$, a vector of size p , and $\mathbf{G}_t = \mathbf{J}_p(1)$ (a Jordan block, which has unit eigenvalue with multiplicity p).

The second order polynomial DLM is related to an important non-parametric tool, namely cubic splines (Wahba, 1990; Green and Silverman, 1993; Eubank, 1999). In Kohn and Ansley (1987), the authors write the spline smoothing formulation of Wahba (1978) as a stochastic difference equation and represent it in the state space form. Therefore, for equally spaced data, it is easy to see that a cubic spline corresponds to a dynamic model with $\mathbf{F} = (1, 0)'$ and $\mathbf{G} = \mathbf{J}_2(1)$. This formulation was further extended to generalized additive regression models by Biller and Fahrmeir (1997).

3.2 Bayesian inference in dynamic Gaussian polynomial models

To facilitate comprehension of the employed method, we devote this subsection to the discussion based on dynamic Gaussian models. In a general framework, we consider the model composed by the observation equation and the state evolution equation

$$y_t = \mathbf{F}_t' \boldsymbol{\theta}_t + \epsilon_t, \quad (4)$$

$$\boldsymbol{\theta}_t = \mathbf{G}_t \boldsymbol{\theta}_{t-1} + \boldsymbol{\omega}_t, \quad (5)$$

where $\epsilon_t \sim N(0, V_t)$ and $\boldsymbol{\omega}_t \sim N(\mathbf{0}, \mathbf{W}_t)$, $t = 1, \dots, T$.

Most of the literature involving state-space dynamic models deals with the Kalman filtering

and smoothing recursions, in order to obtain the joint posterior distributions of the states (for more details, see e.g. West and Harrison, 1997; Kroese and Chan, 2014). This tends to be computationally intensive, so joint sampling directly from $p(\boldsymbol{\theta} | \text{data})$ is more efficient (Carter and Kohn, 1994; Frühwirth-Schnatter, 1994).

In this work we consider the *precision-based algorithm*, a sampling method to obtain the latent states in a single step, avoiding the two steps procedure used by Carter and Kohn (1994) and Frühwirth-Schnatter (1994), and exploiting the sparse feature of precision matrices. This is a scalable procedure and greatly facilitates subsequent aspects of the analysis. The precision-based algorithm has been successfully used by Joshua Chan and collaborators to solve different problems. A few references include some recent papers, like Chan et al. (2013), Chan and Eisenstat (2018), Chan et al. (2020) and Zhang et al. (2020). A seminal work is Chan and Jeliazkov (2009), while interesting and didactic discussions can be found in Chan and Strachan (2012) and Kroese and Chan (2014).

In a brief explanation, one can show that the model in (4)-(5) can be rewritten as

$$\mathbf{y} | \boldsymbol{\theta}, \mathbf{V} \sim N(\mathcal{F}\boldsymbol{\theta}, \mathbf{V}), \quad (6)$$

$$\boldsymbol{\theta} | \boldsymbol{\theta}_0, \mathbf{W} \sim N \left[\boldsymbol{\mathcal{H}}^{-1} \boldsymbol{\mathcal{M}} \boldsymbol{\theta}_0, \left(\boldsymbol{\mathcal{H}}' \mathbf{W}^{-1} \boldsymbol{\mathcal{H}} \right)^{-1} \right], \quad (7)$$

which corresponds to a simple Bayesian regression model, where $\mathbf{y} = (y_1, \dots, y_T)'$, $\mathcal{F} = \text{diag}\{\mathbf{F}'_1, \dots, \mathbf{F}'_T\}$, $\boldsymbol{\theta} = (\boldsymbol{\theta}'_1, \dots, \boldsymbol{\theta}'_T)'$, $\mathbf{V} = \text{diag}\{V_1, \dots, V_T\}$, $\mathbf{W} = \text{diag}\{\mathbf{W}_1, \dots, \mathbf{W}_T\}$, $\boldsymbol{\mathcal{M}} = (\mathbf{G}'_1, \mathbf{0}', \dots, \mathbf{0}')'$ and $\boldsymbol{\mathcal{H}}$ is a block matrix of the form $\boldsymbol{\mathcal{H}}_{ij} = \mathbf{I}$, if $i = j, i = 1, \dots, T$; $-\mathbf{G}_i$, if $i = j - 1, i = 2, \dots, T$; and $\mathbf{0}$, otherwise. It should be noted that (6) and (7) correspond to a Bayesian regression model with a very sparse precision matrix (for details, see Chan and Strachan, 2012).

Due to conjugation, we can easily derive the posterior $\boldsymbol{\theta}|\mathbf{y}, \mathbf{V}, \boldsymbol{\theta}_0, \mathbf{W} \sim N(\bar{\boldsymbol{\mu}}, \bar{\boldsymbol{\Phi}}^{-1})$, where

$$\begin{aligned}\bar{\boldsymbol{\Phi}} &= \mathcal{H}'\mathbf{W}^{-1}\mathcal{H} + \mathcal{F}'\mathbf{V}^{-1}\mathcal{F}, \\ \bar{\boldsymbol{\mu}} &= \bar{\boldsymbol{\Phi}}^{-1}\left(\mathcal{H}'\mathbf{W}^{-1}\mathcal{M}\boldsymbol{\theta}_0 + \mathcal{F}'\mathbf{V}^{-1}\mathbf{y}\right).\end{aligned}$$

One can see that, following the structure of the precision matrix in (7), the posterior precision matrix is also sparse of the band type. The sparseness of the posterior precision matrix allows easily generating the states in a single step, resulting in better efficiency. For this reason, the method is known as precision-based algorithm. The computational advantages of this approach are discussed in more details by McCausland et al. (2011). Moreover, Golub and Van Loan (2013, Chapter 4) discuss the advantages in terms of the number of operations, involving (sparse) band matrices.

3.2.1 Modifying the precision-based algorithm in the polynomial case

Besides the benefits of considering precision-based algorithm as presented above, depending on the model, it can still be improved. For polynomial DLMS, as defined before, the following Markovian structure is implied by the Jordan form:

$$p(\boldsymbol{\vartheta}) = p(\boldsymbol{\vartheta}_1|\boldsymbol{\vartheta}_2) \cdots p(\boldsymbol{\vartheta}_{p-1}|\boldsymbol{\vartheta}_p)p(\boldsymbol{\vartheta}_p), \quad (8)$$

where $\boldsymbol{\vartheta}_k = (\theta_{1k}, \dots, \theta_{Tk})'$, $k = 1, \dots, p$, and $\boldsymbol{\vartheta} = (\boldsymbol{\vartheta}'_1, \dots, \boldsymbol{\vartheta}'_p)'$. We omit the hyperparameters to avoid overloading the notation. Observe that by definition, $\boldsymbol{\vartheta}$ is simply a reordering of $\boldsymbol{\theta}$ in (7), which corresponds to an orthonormal transformation of $\boldsymbol{\theta}$. Therefore, all developments presented before can be easily adapted.

When the modeling is based on polynomial DLMS, it is even possible to preserve the banded property of the precision matrix. For the sake of simplicity, we consider the case of a homoscedastic model with independent innovations, i.e., $V_t \equiv V$ and $\mathbf{W}_t \equiv \mathbf{W} = \text{diag}\{W_1, \dots, W_p\}$, $t = 1, \dots, T$.

This kind of simplification, in (6)-(7), does not provide much computational improvement. However, under the proposed reordering, the Markovian property in (8) provides an additional simplification of model (6)-(7), which is expressed in the proposition below.

Proposition 1. *Let $\boldsymbol{\vartheta}$ be the state vector ordered as in (8). Denote $\mathbf{1} = (1, \dots, 1)'$, a vector of size T , and \mathbf{H} , a $T \times T$ band matrix, which has 1 in its main diagonal, -1 in the sub-diagonal and zero elsewhere. Under the assumption of homoscedasticity with independent innovations, the polynomial DLM can be written as:*

$$\mathbf{y}|\boldsymbol{\vartheta}_1 \sim N(\boldsymbol{\vartheta}_1, V\mathbf{I}), \quad (9)$$

$$\boldsymbol{\vartheta}_k|\boldsymbol{\vartheta}_{k+1} \sim N\left[\boldsymbol{\mu}_k, W_k \left(\mathbf{H}'\mathbf{H}\right)^{-1}\right], k = 1, \dots, p-1, \quad (10)$$

$$\boldsymbol{\vartheta}_p \sim N\left[\boldsymbol{\mu}_p, W_p \left(\mathbf{H}'\mathbf{H}\right)^{-1}\right], \quad (11)$$

where $\boldsymbol{\mu}_k = (\theta_{0k} + \theta_{0(k+1)})\mathbf{1} + (\mathbf{H}^{-1} - \mathbf{I})\boldsymbol{\vartheta}_{k+1}$, $k = 1, 2, \dots, p-1$, and $\boldsymbol{\mu}_p = \theta_{0p}\mathbf{1}$.

The model above makes clear the Markovian property (8). Furthermore, the model in (9)-(11) is similar to the model in (6)-(7), with the same features of sparseness and band type, representing a simple regression with a special prior. Observe that the mean of $\mathbf{y}|\boldsymbol{\vartheta}_1$ in (9) does not need any operation after the reordering. Moreover, instead of dealing with vectors and matrices of order pT , we simplify by working with p vectors and matrices (also sparse) of order T in (10) and (11).

The full conditional posterior distributions of the vectors $\boldsymbol{\vartheta}_k$, $k = 1, 2, \dots, p$, are easier to handle than in the full vector $\boldsymbol{\vartheta}$. In order to simplify notations, we denote $\mathbf{B} = \mathbf{I} - \mathbf{H}$. Therefore,

$$\boldsymbol{\vartheta}_k|[\dots] \sim N(\bar{\boldsymbol{\mu}}_k, \bar{\boldsymbol{\Phi}}_k^{-1}), \quad (12)$$

where the precision matrix and the mean vector are, respectively,

$$\bar{\boldsymbol{\Phi}}_k = \begin{cases} \frac{1}{V}\mathbf{I} + \frac{1}{W_1}\mathbf{H}'\mathbf{H}, & \text{if } k = 1, \\ \frac{1}{W_{k-1}}\mathbf{B}'\mathbf{B} + \frac{1}{W_k}\mathbf{H}'\mathbf{H}, & \text{if } k = 2, 3, \dots, p, \end{cases}$$

and

$$\bar{\boldsymbol{\mu}}_k = \begin{cases} \bar{\Phi}_1^{-1} \left[\frac{1}{V} \mathbf{y} + \frac{\theta_{01} + \theta_{02}}{W_1} \mathbf{e}_1 + \frac{1}{W_1} \mathbf{H}' \mathbf{B} \boldsymbol{\vartheta}_2 \right], & \text{if } k = 1, \\ \bar{\Phi}_k^{-1} \left[\frac{1}{W_{k-1}} \mathbf{B}' \mathbf{H} \boldsymbol{\vartheta}_{k-1} + \frac{\theta_{0k} + \theta_{0(k+1)}}{W_k} \mathbf{e}_1 + \frac{1}{W_k} \mathbf{H}' \mathbf{B} \boldsymbol{\vartheta}_{k+1} \right], & \text{if } k = 2, 3, \dots, p-1, \\ \bar{\Phi}_p^{-1} \left[\frac{1}{W_{p-1}} \mathbf{B}' \mathbf{H} \boldsymbol{\vartheta}_{p-1} + \frac{\theta_{0p}}{W_p} \mathbf{e}_1 \right], & \text{if } k = p. \end{cases}$$

Although it looks complicated, the sequential structure is simple to implement and can be easily generalized to the case where the data are not normally distributed, more efficiently than in model (6)-(7).

It remains to discuss the initial values θ_{0k} and the variances V and W_k , $k = 1, 2, \dots, p$. We assume independent priors. With respect to the initial values, if we consider the priors $\theta_{0k} \sim N(\mu_{\theta_{0k}}, \sigma_{\theta_{0k}}^2)$, it is easy to see that the full conditional posterior is

$$\theta_{0k} | [\dots] \sim N(\bar{\mu}_{0k}, \bar{\sigma}_{0k}^2), \quad (13)$$

where

$$\bar{\sigma}_{0k}^2 = \begin{cases} \left(\frac{1}{\sigma_{01}^2} + \frac{1}{W_1} \right)^{-1}, & \text{if } k = 1; \\ \left(\frac{1}{\sigma_{0k}^2} + \frac{1}{W_{k-1}} + \frac{1}{W_k} \right)^{-1}, & \text{if } k = 2, 3, \dots, p; \end{cases}$$

and

$$\bar{\mu}_{0k} = \begin{cases} \bar{\sigma}_{01}^2 \left(\frac{\mu_{01}}{\sigma_{01}^2} + \frac{\theta_{11} - \theta_{02}}{W_1} \right), & \text{if } k = 1; \\ \bar{\sigma}_{0k}^2 \left(\frac{\mu_{0k}}{\sigma_{0k}^2} + \frac{\theta_{1(k-1)} - \theta_{0(k-1)}}{W_{k-1}} + \frac{\theta_{1k} - \theta_{0(k+1)}}{W_k} \right), & \text{if } k = 2, 3, \dots, p-1; \\ \bar{\sigma}_{0p}^2 \left(\frac{\mu_{0p}}{\sigma_{0p}^2} + \frac{\theta_{1(p-1)} - \theta_{0(p-1)}}{W_{k-1}} + \frac{\theta_{1p}}{W_p} \right), & \text{if } k = p. \end{cases}$$

Instead of working with variances, we consider the precisions $1/V$ and $1/W_k$. Thus, assume that $W_k^{-1} \sim \Gamma(\nu_{0k}, \eta_{0k})$. One can see that the full conditional posterior is

$$W_k^{-1} | [\dots] \sim \Gamma(\bar{\nu}_{0k}, \bar{\eta}_{0k}), \quad (14)$$

with parameters

$$\begin{aligned}\bar{\nu}_{0k} &= \nu_{0k} + \frac{T}{2}, \\ \bar{\eta}_{0k} &= \eta_{0k} + \frac{1}{2}(\boldsymbol{\vartheta}_k - \boldsymbol{\mu}_k)' \mathbf{H}' \mathbf{H} (\boldsymbol{\vartheta}_k - \boldsymbol{\mu}_k),\end{aligned}$$

where $\boldsymbol{\mu}_k$ is the same in (10)-(11) for $k = 1, 2, \dots, p$.

Similarly, if $V^{-1} \sim \Gamma(\nu_y, \eta_y)$, then

$$V^{-1}[[\dots]] \sim \Gamma(\bar{\nu}_y, \bar{\eta}_y), \tag{15}$$

where

$$\begin{aligned}\bar{\nu}_y &= \nu_y + \frac{T}{2}, \\ \bar{\eta}_y &= \eta_y + \frac{1}{2} \sum_{t=1}^T (y_t - \theta_{t1})^2.\end{aligned}$$

All the posteriors above are conjugated, which allows the use of the Gibbs algorithm. In the next section, we deal with the case where the relationship between observation and state equations is nonlinear, which encompasses as a special case the dynamic mixture weights. This situation demands more computational efforts and our approach tends to simplify the development of the method.

The derivation of the results presented in this subsection is available in the supplementary material.

3.3 Bayesian inference in nonlinear dynamic models

In the case where the data are not normally distributed or the relationship between observation and state equations is nonlinear, Chan and collaborators proposed extensions to the precision-based algorithm (see, e.g., Chan et al., 2013). The idea is to apply the accept-reject Metropolis-Hastings

(ARMH) algorithm (see Chib and Greenberg, 1995) to the whole vector of states. This method is described in more details in Chan and Strachan (2012).

Another benefit of considering the reordering of the vector of states, as proposed in Section 3.2, is the ability to deal with nonlinear dynamic models. The main reason is that extensions like those cited above tend to be more computationally intensive. Therefore, the smaller the vector of states is, the better. Thus, instead of dealing with the whole vector of states as in the approach of Chan and collaborators, in our proposal one can deal with only the first component of the state vector, $\boldsymbol{\vartheta}_1$. The remaining vectors $\boldsymbol{\vartheta}_k$, $k = 2, 3, \dots, p$, will have full conditional posteriors as in (12), which is more easily calculated.

One problem of considering the ARMH algorithm as presented in Chan and Strachan (2012) and Chan et al. (2013) is that, depending on the complexity (e.g., the distribution of the observed data and/or the size T of the series), the algorithm tends to have difficulties in providing a good acceptance rate, which might interfere in the performance of the MCMC. In a few numerical experiments (not reported here), involving “simple cases” of Bernoulli data, the algorithm was problematic. Because of this issue, and exploiting an interesting property of the joint (prior) distribution of $\boldsymbol{\vartheta}_1$, we consider two alternatives in this work: (i) the component-wise Metropolis-Hastings (CWMH) algorithm (MH algorithm for each element of $\boldsymbol{\vartheta}_1$); and (ii) for the specific case of Bernoulli data, the use of the probit link function. The latter case is not as general as the former, but is useful to estimate the dynamic mixture weights.

In a general situation, let the likelihood function be written as $p(\mathbf{y}|\boldsymbol{\alpha}) = \prod_{t=1}^n p(y_t|\alpha_t)$. Also, assume that there exists a (link) function $\mathcal{T} : A \rightarrow \mathbb{R}$, which is continuous and bijective, where A corresponds to the parameter space of the α_t 's. Thus, once the full conditional posterior of $\boldsymbol{\vartheta}_1$ is drawn, one can have $\alpha_t = \mathcal{T}^{-1}(\theta_{t1})$, where \mathcal{T}^{-1} denotes the inverse function of \mathcal{T} .

3.3.1 Component-wise Metropolis-Hastings

The idea of CWMH might look computationally intensive. However, when dealing with polynomial DLMS, several calculations are simplified. An interesting property that can be used, closely related to results in Rue and Held (2005), is presented below.

Theorem 1. Let $\boldsymbol{\vartheta}_1$ be defined as in (8) and denote $\boldsymbol{\vartheta}_{(t)1} = (\theta_{11}, \dots, \theta_{t-1,1}, \theta_{t+1,1}, \dots, \theta_{T1})'$. Thus

$$\theta_{t1} | \boldsymbol{\vartheta}_{(t)1}, \boldsymbol{\vartheta}_2 \sim N(\mu_{t1}^*, \tau_t^2),$$

where

$$\mu_{t1}^* = \begin{cases} \frac{1}{2} [(\theta_{t+1,1} - \theta_{t2}) + (\theta_{t-1,1} + \theta_{t-1,2})], & \text{if } t = 1, \dots, T-1, \\ \theta_{T-1,1} + \theta_{T-1,2}, & \text{if } t = T, \end{cases}$$

and

$$\tau_t^2 = \begin{cases} \frac{W_t}{2}, & \text{if } t = 1, \dots, T-1, \\ W_T, & \text{if } t = T. \end{cases}$$

By this theorem, it is clear that the conditional distribution of $\theta_{t1} | \boldsymbol{\vartheta}_{(t)1}, \boldsymbol{\vartheta}_2$ demands only $O(T)$ operations, showing how simplified the process can be. Furthermore, observe that μ_{t1}^* above can be seen as a prediction for θ_{t1} . For $t = 1, \dots, T-1$, so it is an average of conditional expectations of θ_{t1} in the t -th and $(t+1)$ -th equations in the local level, whereas μ_{T1}^* can be interpreted as a conditional expectation of θ_{T1} in the T -th equation. The proof of the theorem is available in the supplementary material.

Thus, based on Theorem 1, one can derive the full conditional posterior distribution as

$$p(\theta_{t1} | [\dots]) \propto \varphi(\theta_{t1} | \mu_{t1}^*, \tau_t^2) p(y_t | \mathcal{T}^{-1}(\theta_{t1})), \quad t = 1, 2, \dots, T,$$

where $\varphi(x|a, b)$ denotes the probability density function of a normal r.v. with mean a and variance b , evaluated at x . Observe by the posterior above that the CWMH is quite general and fits to any nonlinear case, with any (bijective) link function \mathcal{T} .

As a proposed distribution, we consider a random walk, with variance adapted during the MCMC iterations as in Roberts and Rosenthal (2009). Then, for each $t = 1, 2, \dots, T$, one can draw a candidate $\theta_{t1}^* \sim N(\theta_{t1}, \zeta_t^2)$, which will or will not be accepted in a Metropolis-Hastings procedure. The variance ζ_t^2 can be increased/reduced in order to ensure an acceptance rate of 0.44. Basically, during the MCMC, after the n -th “batch” of 50 iterations, the authors suggest adding or subtracting the standard deviation in log-scale by $\min(0.01, n^{-1/2})$. For more details, see the aforementioned reference.

3.3.2 The probit link for Bernoulli data

For the specific case of Bernoulli data, one can also consider another efficient way of sampling the α_t 's almost jointly. One can consider the probit link function to apply the proposal of Albert and Chib (1993).

Here we consider $\mathcal{T} \equiv \Phi^{-1}$, the inverse of the cumulative distribution function of a standard normal r.v. Basically, we have that $\alpha_t = \Phi(\theta_{t1})$, $t = 1, 2, \dots, T$. The trick consists of writing α_t in a GLM context, where the “design matrix” is an identity of order T , denoted by \mathbf{I} .

In this case, there exist T latent r.v.'s v_1, v_2, \dots, v_T , where the v_t 's are independent, with $v_t \sim N(\theta_{t1}, 1)$, such that $y_t = 1$ if $v_t > 0$, and $y_t = 0$ otherwise. Thus, one can see that $\alpha_t = \mathbb{P}(y_t = 1) = \Phi(\theta_{t1})$. Therefore, based on (10), it is easy to see that

$$\begin{aligned} v_t | y_t = 0, \theta_{t1} &\sim N(\theta_{t1}, 1) \text{ truncated at the right by } 0, \\ v_t | y_t = 1, \theta_{t1} &\sim N(\theta_{t1}, 1) \text{ truncated at the left by } 0. \end{aligned}$$

The full conditional posterior for $\boldsymbol{\vartheta}_1$ is

$$\boldsymbol{\vartheta}_1 | \mathbf{v}, [\dots] \sim N(\bar{\boldsymbol{\mu}}_1, \bar{\boldsymbol{\Phi}}_1^{-1}), \tag{16}$$

where

$$\begin{aligned}\bar{\Phi}_1 &= \mathbf{I} + \frac{1}{W_1} \mathbf{H}' \mathbf{H}, \\ \bar{\boldsymbol{\mu}}_1 &= \bar{\Phi}_1^{-1} \left[\mathbf{v} + \frac{\theta_{01} + \theta_{02}}{W_1} \mathbf{e}_1 + \frac{1}{W_1} \mathbf{H}' \mathbf{B} \boldsymbol{\vartheta}_2 \right],\end{aligned}$$

with $\mathbf{v} = (v_1, v_2, \dots, v_T)'$. Compare the similarity of (16) with (12). Basically, the full conditional posterior of $\boldsymbol{\vartheta}_1$ here has one more step, which corresponds to the generation of the latent variables \mathbf{v} . The consequence is an algorithm almost as efficient as in the case of the dynamic Gaussian linear model.

3.4 Bayesian estimation of the dynamic mixture weights

The development in Section 3.3 is fundamental for the estimation of the weights α_t 's in the dynamic Gaussian mixture problem. As mentioned before, in the dynamic case, $z_t \sim \text{Bern}(\alpha_t)$, $t = 1, \dots, T$. Based on item (iii) in Section 2.1, it is easy to generalize and see that the full conditional posterior can be written as

$$z_t | y_t, [\dots] \sim \text{Bern}(\alpha_t^*), \quad (17)$$

where $\alpha_t^* = \frac{\alpha_t \varphi(y_t | \mu_2, \phi_2^{-1})}{(1 - \alpha_t) \varphi(y_t | \mu_1, \phi_1^{-1}) + \alpha_t \varphi(y_t | \mu_2, \phi_2^{-1})}$, $t = 1, 2, \dots, T$.

Once the latent categorical variables z_t 's are generated, one can proceed to estimate the α_t 's as in the nonlinear dynamic model, with a Bernoulli response. Therefore, the full conditional posterior of the dynamic mixture weights can be derived according to the procedures described in Sections 3.3.1 and 3.3.2. In the former case, a natural candidate as link function is the logit, where $\text{logit}(x) = \log[x/(1 - x)]$, for $0 < x < 1$.

3.4.1 Gibbs sampling algorithm

Once we have in hand the full conditional posterior distributions, we can generate the MCMC for the problem. Thus, posterior draws can be obtained by sequentially sampling as below:

1. Generate the means and precisions of the mixture parameters (μ_k, ϕ_k) , $k = 1, 2$, as in (2) and (3). After generation, order the pairs under the constraint $\mu_1 < \mu_2$;
2. Generate an independent sample of z_t , $t = 1, 2, \dots, T$, as in (17);
3. For k from p to 2:
 - (a) Generate θ_{0k} as in (13);
 - (b) Generate W_k as in (14);
 - (c) Generate $\boldsymbol{\vartheta}_k$ as in (12);
4. Generate θ_{01} as in (13);
5. Generate W_1 as in (14);
6. Generate $\boldsymbol{\vartheta}_1$ as in Section 3.3.1 for the logit link, or Section 3.3.2 for the probit link (using the categorical z_t 's instead of y_t 's in the refereed se sections);
7. Calculate $\alpha_t = \mathcal{T}^{-1}(\theta_{t1})$, $t = 1, 2, \dots, T$.

4 Synthetic data

In this section we evaluate the performance of the method proposed in Section 3 using simulated data. Motivated by the arguments in Section 3.1, second-order dynamic polynomial models are considered for this task. We give emphasis to binomial models, concluding with some Gaussian mixture models. In both cases, the probability of success and the mixture weight evolve over time, following traditional patterns found in the literature.

We focus on the diversity of shapes, in order to see how the method performs under different scenarios. Therefore, we consider four different dynamic behaviors for α_t , which are presented here

scaled in the unit interval:

(1) Linear behavior: $\alpha_t^{(1)} = 0.1 + 0.8t$;

(2) Parabolic behavior: $\alpha_t^{(2)} = 3(t - 0.5)^2 + 0.125$;

(3) Sinusoidal behavior: $\alpha_t^{(3)} = \cos(2\pi(t + \pi))/2.5 + 0.5$;

(4) Stepwise behavior: $\alpha_t^{(4)} = 0.2\mathbb{1}_{[0,0.3)}(t) + 0.8\mathbb{1}_{[0.3,0.7)}(t) + 0.3\mathbb{1}_{[0.7,1)}(t)$, where $\mathbb{1}_A(t)$ is an indicator function, which is one, if $t \in A$, and zero, otherwise.

The initial information of the state equations, defined as θ_{01} and θ_{02} , is described through independent normal distributions with mean zero and variance one, which is enough to provide a relatively vague initial information regarding α_1 (the probability of instant one). In other words, after applying the transformation (logit or probit), one can have the initial probability of the α_t 's in a range close to the unit interval.

Unlike Biller and Fahrmeir (1997), we simplify the structure of the precision innovations by taking into account independent priors of the form

$$1/W_1 \sim \Gamma(0.01, 0.01),$$

$$1/W_2 \sim \Gamma(0.01, 0.01).$$

These two priors will provide precision parameters with mean 1 and variance 100.

The MCMC chains were developed with 220,000 iterations for each parameter. From these chains we discarded a burn-in of size 20,000 and took observations with a lag of size 200, resulting in a final chain of 1,000 values. The point estimates considered here are the medians (based on the absolute risk).

4.1 Binomial data

In order to explore the ability of the method to estimate the α_t 's, in this first study we consider binomial datasets, with a fixed number of Bernoulli trials. This study is useful to observe how well the method can estimate the α_t 's. For the sake of comparison, we also generate a normal dataset with mean being the probabilities. Therefore, we considered four distributions: $\text{bin}(n, \alpha_t)$ with $n = 1, 15, 30$; and $N(\alpha_t, 0.1^2)$. For each distribution, we generated datasets using α_t with behaviors (1)–(4), as previously defined. The variance used for the normal data was chosen so that the behavior of the normal observations would be similar to the binomial data, such as $\text{bin}(30, \alpha_t)$.

Three sample sizes were employed: $T = 200, 400, 800$. Since the qualitative results were similar, we present here only the case where $T = 400$. The datasets are presented in Figure 1, where the rows represent data generated according to each function $\alpha_t^{(1)} - \alpha_t^{(4)}$. Moreover, the columns 1 – 4 correspond to the distribution employed. Two things can be clearly observed: (i) the binomial dataset indeed tends to look similar to the normal dataset as the number of Bernoulli trials increases; and (ii) the Bernoulli dataset (first column), unlike the others, do not show any pattern of similarity to α_t , which makes it challenging to fit a model.

[Figure 1 about here.]

After generated the dataset, MCMC chains were run and the α_t 's were estimated using the Gibbs sampling algorithm presented in Section 3.4.1. Since this first simulated data study does not take into account the mixture problem, the MCMC chains were developed using only steps 3 – 7 in the aforementioned section. The transform employed for the binomial dataset was the logit, since the probit function, as considered in Section 3.3.2, is only appropriate for binary data. With respect to the normal dataset, we considered the posterior (12) with identity link function; and for the precision of the observations, the posterior (15), based on the prior $1/V \sim \Gamma(0.01, 0.01)$.

The point estimates are presented in Figure (2). One can see that the method tends to provide good estimates. The data from $bin(30, \alpha_t)$ and $N(\alpha_t, 0.1^2)$ provide the best results, which makes sense. Indeed, these data have clear shape of the function of interest, which makes the task basically a simple denoising problem. On the other hand, although it is not possible to obtain estimates for the Bernoulli dataset as good as the others, one can see good performance. In this case, the simplicity of the data makes the problem even more complex, because binary data do not provide good knowledge about the dynamics of the α_t 's. The simple fact that the shape of the estimates is similar to that of the real curves indicates how promising is the idea of using the proposed approach in the context of mixture problems.

[Figure 2 about here.]

Continuing the comparison, we can also evaluate the performance of the probit function in the case of the Bernoulli datasets. The estimates using logit and probit are presented in Figure 3. One can see that the estimates under these two transforms are similar. Furthermore, it is important to mention the fact that it is possible to find conjugacy when we use the probit function, which makes the generation of the chains faster than when we apply the CWMH algorithm to the elements of the vector $\boldsymbol{\vartheta}_1$.

[Figure 3 about here.]

4.2 Mixture data

After observing the performance of the proposed method for binomial data, we can combine the development for the case where the datasets are mixtures. In this study we focus on the mixture of two normally distributed groups of the kind

$$y_t = (1 - z_t)x_{1t} + z_t x_{2t},$$

where $z_t|\alpha_t \sim \text{Bern}(\alpha_t)$, $x_{1t} \sim N(0, 0.25)$, $x_{2t} \sim N(2, 0.25)$ (which means $\phi_1 = \phi_2 = 4$). With respect to α_t , we also consider here the cases of $\alpha_t^{(k)}$, $t = 1, 2, \dots, T$, $k = 1, 2, 3, 4$ described at the beginning of the section. As in Section 4.1, we generated datasets of sizes $T = 200, 400, 800$. Also here, the results were similar, so we present only the case where $T = 400$.

The data generated are presented in Figure 4. Observe the complexity of identifying the real dynamic mixture weights, even with the groups being highlighted, which does not happen in practice.

[Figure 4 about here.]

With respect to the priors for the component parameters, we considered $\mu_1 \sim N(q_1, 10s^2)$, $\phi_1 \sim \Gamma(0.01, 0.01)$, $\mu_2 \sim N(q_3, 10s^2)$ and $\phi_2 \sim \Gamma(0.01, 0.01)$, where q_1 and q_3 correspond to the 1st and 3rd quartile of the observed data, respectively, and s^2 represents the sample variance. We maintained the same prior applied for other precision parameters. Moreover, the priors for the means are relatively vague, with their means respecting the amplitude of the data. In this scenario, the proposed priors also took into account the constraint to avoid label switching (step 1 of Section 3.4.1).

For the generated mixture data, according to each mixture weight $\alpha^{(1)} - \alpha^{(4)}$, MCMC chains were run by the Gibbs algorithm indicated in Section 3.4.1. We considered both link functions, probit and logit, in the estimation of the α_t 's.

The estimates of the mixture weights are presented in Figure (5). One can see that the proposed method tends to provide good estimates, with shape that mimics the real curves. Furthermore, the estimates provided using probit and logit link functions are similar.

[Figure 5 about here.]

The performance of the method to estimate the component parameters is presented in Table

1. One can see that the results using both link functions, logit and probit, are very similar. The method presents good point estimates, and most of the parameters belong to the 90% HPD credible intervals. For the data generated using mixture weights with step behavior, the CI's of μ_1 failed to contain the true value (using both, logit and probit, link functions), as well as for μ_2 in the case of using the logit. This happens most likely due to randomness. Although it is not presented here, we also estimated 95% HPD credible intervals, where this issue was no longer observed.

[Table 1 about here.]

5 Application to the glioblastoma multiforme dataset

The glioblastoma multiforme (GBM) dataset is related to a malignant tumor. The patient survival time for this kind of cancer has a median time of one year. The observations of the data are known as *array Comparative Genomic Hybridization* (aCGH). They correspond to log-ratios of normalized intensities from disease *vs.* control samples, which are indexed by the physical location of the probes on the genome (Lai et al., 2005). In other words, large values of aCGH suggest chromosomal aberrations in the specified locations. For this reason, the detection of regions with high proportions of abnormalities can be critical to comprehend the pathogenesis.

The data are presented in Figure 6. They correspond to $n = 193$ aCGH observations. In this application we consider a mixture problem, where the observations can be treated as normal or aberrations. A similar study was performed by Montoril et al. (2019). In their proposal, the authors needed to assume that the groups have known means, but in the application they had to estimate these parameters by averages and treat them as if they were the “real” ones. In the present paper, we estimate jointly both, the dynamic mixture weights and the mixture component parameters. Furthermore, credible intervals can also be provided, unlike in the aforementioned

paper.

[Figure 6 about here.]

In order to apply the proposed method to the data, we considered the same priors adopted in Section 4.2, and a second-order polynomial nonlinear dynamic model to estimate the mixture weights. We also adopted the same MCMC setup used in the previous section and we modeled the aCGH dataset using logit and probit link functions. Based on the MCMC results of the component parameters, estimates are summarized in Table 2, where one can see similar results using both link functions. Also using these MCMC data, the behavior of the distribution of the posteriors is presented in Figure 7. The use of the logit or probit link function tends to provide posterior distributions that are very similar. A little more variability can be seen when the probit link function is adopted.

[Table 2 about here.]

[Figure 7 about here.]

With respect to the mixture weights, estimates are presented in Figure 8. Both HPD intervals are very tight, ensuring high precision for the point estimates. The use of the logit link function provides point estimates that suggest the existence of four regions with chromosome aberrations. Although it is not so easily seen, due to the tightness of the third peak and its proximity to the fourth, the 90% HPD credible intervals reinforce the conclusion that there are four regions with chromosome aberrations (the lower limit for the third peak is around 0.8). When using the probit link function, the existence of four peaks is observed with high probability. These results presented are inline with the literature (see Lai et al., 2005).

[Figure 8 about here.]

In comparison with Montoril et al. (2019), the present proposal was able to detect the peaks with higher probabilities. Also, the third and fourth peaks presented here are in the same region as the third peak in the previous paper. The high probability presented by our method indicates the possibility of indices that can be better investigated.

The method is good to detect amplifications because the groups are separable. This makes it easier for the model to detect the groups clearly. Hence, the component parameter estimates tend to be unbiased, which in turn helps the estimation of the dynamic mixture weights.

6 Conclusions and further remarks

In this work we propose, to the best of our knowledge, a new method to deal with Gaussian mixture models, where the mixture weights are allowed to have a dynamic behavior. The problem was studied with the use of polynomial dynamic models. We explored and developed properties for these models based on the ideas of Chan and Jeliazkov (2009).

A general method, which can consider the estimation of the dynamic mixture weights as a particular case, was explored here, where two possibilities were considered, namely: (i) component-wise Metropolis-Hastings; and (ii) probit link function for Bernoulli data. In (ii), a probit link function was used to efficiently estimate dynamic curves. In (i), the method was able to use any (bijective) link function (we used the logit), although it was not as fast as (ii). In the simulation studies and in the application, both proposals provided similar results, with a little more variability of results based on (ii).

Due to the complexity of the problem and the its wide applicability, we focused on the case of a dynamic mixture of two normal distributions. The general case encompasses $K \geq 2$ groups for the Gaussian mixture model and will be left as topic of future research.

Another topic for future research is a scalable version of the dynamic generalized linear model, following West et al. (1985). This is a combination of variational Bayes ideas with linear Bayes estimation. Two advantages of this approach are the recovery of sequential analysis, which allows for subjective intervention and faster processing time.

Acknowledgements

We are grateful to Dr. Daiane A. Zuanetti, from the Department of Statistics at Federal University of São Carlos, for the discussions and suggestions about mixture models. The first author acknowledges FAPESP (Fundação de Amparo à Pesquisa do Estado de São Paulo) for the grant 2018/04654-9. The third author acknowledges FAPESP for the grant 1032, to visit the University of Campinas, and FAPERJ (Fundação de Amparo à Pesquisa do Estado do Rio de Janeiro) for the grant E-26/007/10667/2019.

Supplementary material

Proofs of the results presented in Section 3.

References

- Albert, J. H. and Chib, S. (1993). Bayesian Analysis of Binary and Polychotomous Response Data. *Journal of the American Statistical Association*, 88(422):669–679.
- Billier, C. and Fahrmeir, L. (1997). Bayesian Spline-Type Smoothing in Generalized Regression Models. *Computational Statistics*, 12(2):1–16.

- Bouguila, N. and Fan, W., editors (2020). *Mixture Models and Applications*. Unsupervised and Semi-Supervised Learning. Springer International Publishing, Cham.
- Boys, R. J. and Henderson, D. A. (2004). A Bayesian Approach to DNA Sequence Segmentation. *Biometrics*, 60(3):573–581.
- Carter, C. K. and Kohn, R. (1994). On Gibbs sampling for state space models. *Biometrika*, 81(3):541–553.
- Chan, J. C., Eisenstat, E., and Strachan, R. W. (2020). Reducing the state space dimension in a large TVP-VAR. *Journal of Econometrics*, 218(1):105–118.
- Chan, J. C. C. and Eisenstat, E. (2018). Bayesian model comparison for time-varying parameter VARs with stochastic volatility. *Journal of Applied Econometrics*, 33(4):509–532.
- Chan, J. C. C. and Jeliazkov, I. (2009). Efficient simulation and integrated likelihood estimation in state space models. *International Journal of Mathematical Modelling and Numerical Optimisation*, 1(1/2):101–120.
- Chan, J. C. C., Koop, G., and Potter, S. M. (2013). A New Model of Trend Inflation. *Journal of Business & Economic Statistics*, 31(1):94–106.
- Chan, J. C. C. and Strachan, R. W. (2012). Estimation in Non-Linear Non-Gaussian State Space Models with Precision-Based Methods. CAMA Working Papers 2012-13, Centre for Applied Macroeconomic Analysis, Crawford School of Public Policy, The Australian National University.
- Chib, S. and Greenberg, E. (1995). Understanding the Metropolis-Hastings Algorithm. *The American Statistician*, 49(4):327–335.

- Escobar, M. D. and West, M. (1995). Bayesian Density Estimation and Inference Using Mixtures. *Journal of the American Statistical Association*, 90(430):577–588.
- Eubank, R. L. (1999). *Nonparametric regression and spline smoothing*, volume 157 of *Statistics, textbooks and monographs*. Chapman & Hall, New York, 2nd edition.
- Fahrmeir, L. and Tutz, G. (2001). State Space and Hidden Markov Models. In *Multivariate Statistical Modelling Based on Generalized Linear Models*, pages 331–383. Springer New York, New York, 2nd edition. Series Title: Springer Series in Statistics.
- Fernando, B., Fromont, E., Muselet, D., and Sebban, M. (2012). Supervised learning of Gaussian mixture models for visual vocabulary generation. *Pattern Recognition*, 45(2):897–907.
- Frühwirth-Schnatter, S. (1994). DATA AUGMENTATION AND DYNAMIC LINEAR MODELS. *Journal of Time Series Analysis*, 15(2):183–202.
- Frühwirth-Schnatter, S. (2006). *Finite mixture and Markov switching models*. Springer series in statistics. Springer, New York. OCLC: ocm71262594.
- Golub, G. H. and Van Loan, C. F. (2013). *Matrix computations*. Johns Hopkins studies in the mathematical sciences. The Johns Hopkins University Press, Baltimore, 4th edition. OCLC: ocn824733531.
- Green, P. J. and Silverman, B. W. (1993). *Nonparametric Regression and Generalized Linear Models: A roughness penalty approach*, volume 58 of *Monographs on Statistics & Applied Probability*. Chapman and Hall/CRC, New York.
- Hastie, T., Tibshirani, R., and Friedman, J. H. (2017). *The elements of statistical learning : data mining, inference, and prediction*. Springer Series in Statistics. Springer, New York, 2nd edition.

- Holsclaw, T., Greene, A. M., Robertson, A. W., and Smyth, P. (2017). Bayesian nonhomogeneous Markov models via Pólya-Gamma data augmentation with applications to rainfall modeling. *The Annals of Applied Statistics*, 11(1):393–426.
- Kohn, R. and Ansley, C. F. (1987). A New Algorithm for Spline Smoothing Based on Smoothing a Stochastic Process. *SIAM Journal on Scientific and Statistical Computing*, 8(1):33–48.
- Kroese, D. P. and Chan, J. C. C. (2014). *Statistical Modeling and Computation*. Springer, New York.
- Lai, W. R., Johnson, M. D., Kucherlapati, R., and Park, P. J. (2005). Comparative analysis of algorithms for identifying amplifications and deletions in array CGH data. *Bioinformatics*, 21(19):3763–3770.
- McCausland, W. J., Miller, S., and Pelletier, D. (2011). Simulation smoothing for state–space models: A computational efficiency analysis. *Computational Statistics & Data Analysis*, 55(1):199–212.
- Meligkotsidou, L. and Dellaportas, P. (2011). Forecasting with non-homogeneous hidden Markov models. *Statistics and Computing*, 21(3):439–449.
- Montoril, M. H., Pinheiro, A., and Vidakovic, B. (2019). Wavelet-based estimators for mixture regression. *Scandinavian Journal of Statistics*, 46(1):215–234.
- Raymond, J. E. and Rich, R. W. (1997). Oil and the Macroeconomy: A Markov State-Switching Approach. *Journal of Money, Credit and Banking*, 29(2):193.
- Richardson, S. and Green, P. J. (1997). On Bayesian Analysis of Mixtures with an Unknown Number of Components (with discussion). *Journal of the Royal Statistical Society: Series B (Statistical Methodology)*, 59(4):731–792.

- Robert, C. P., Ryden, T., and Titterton, D. M. (2000). Bayesian inference in hidden Markov models through the reversible jump Markov chain Monte Carlo method. *Journal of the Royal Statistical Society: Series B (Statistical Methodology)*, 62(1):57–75.
- Roberts, G. O. and Rosenthal, J. S. (2009). Examples of Adaptive MCMC. *Journal of Computational and Graphical Statistics*, 18(2):349–367.
- Rue, H. and Held, L. (2005). *Gaussian Markov random fields: theory and applications*. Number 104 in Monographs on statistics and applied probability. Chapman & Hall/CRC, Boca Raton.
- Saraiva, E. F. and Milan, L. A. (2012). Clustering Gene Expression Data using a Posterior Split-Merge-Birth Procedure: Clustering gene expression data. *Scandinavian Journal of Statistics*, 39(3):399–415.
- Spezia, L. (2010). Bayesian analysis of multivariate Gaussian hidden Markov models with an unknown number of regimes: BAYESIAN ANALYSIS OF HIDDEN MARKOV MODELS. *Journal of Time Series Analysis*, 31(1):1–11.
- Spezia, L. (2020). Bayesian variable selection in non-homogeneous hidden Markov models through an evolutionary Monte Carlo method. *Computational Statistics & Data Analysis*, 143:106840.
- Tobias Rydén, Timo Teräsvirta, and Stefan Åsbrink (1998). Stylized facts of daily return series and the hidden Markov model. *Journal of Applied Econometrics*, 13(3):217–244.
- Wahba, G. (1978). Improper Priors, Spline Smoothing and the Problem of Guarding Against Model Errors in Regression. *Journal of the Royal Statistical Society. Series B (Methodological)*, 40(3):364–372.
- Wahba, G. (1990). *Spline Models for Observational Data*, volume 59 of *CBMS-NSF Regional Conference Series in Applied Mathematics*. Society for Industrial and Applied Mathematics.

West, M. and Harrison, J. (1997). *Bayesian forecasting and dynamic models*. Springer series in statistics. Springer, New York, 2nd ed edition.

West, M., Harrison, P. J., and Migon, H. S. (1985). Dynamic Generalized Linear Models and Bayesian Forecasting. *Journal of the American Statistical Association*, 80(389):73–83.

Zhang, B., Chan, J. C., and Cross, J. L. (2020). Stochastic volatility models with ARMA innovations: An application to G7 inflation forecasts. *International Journal of Forecasting*, pages 1318–1328.

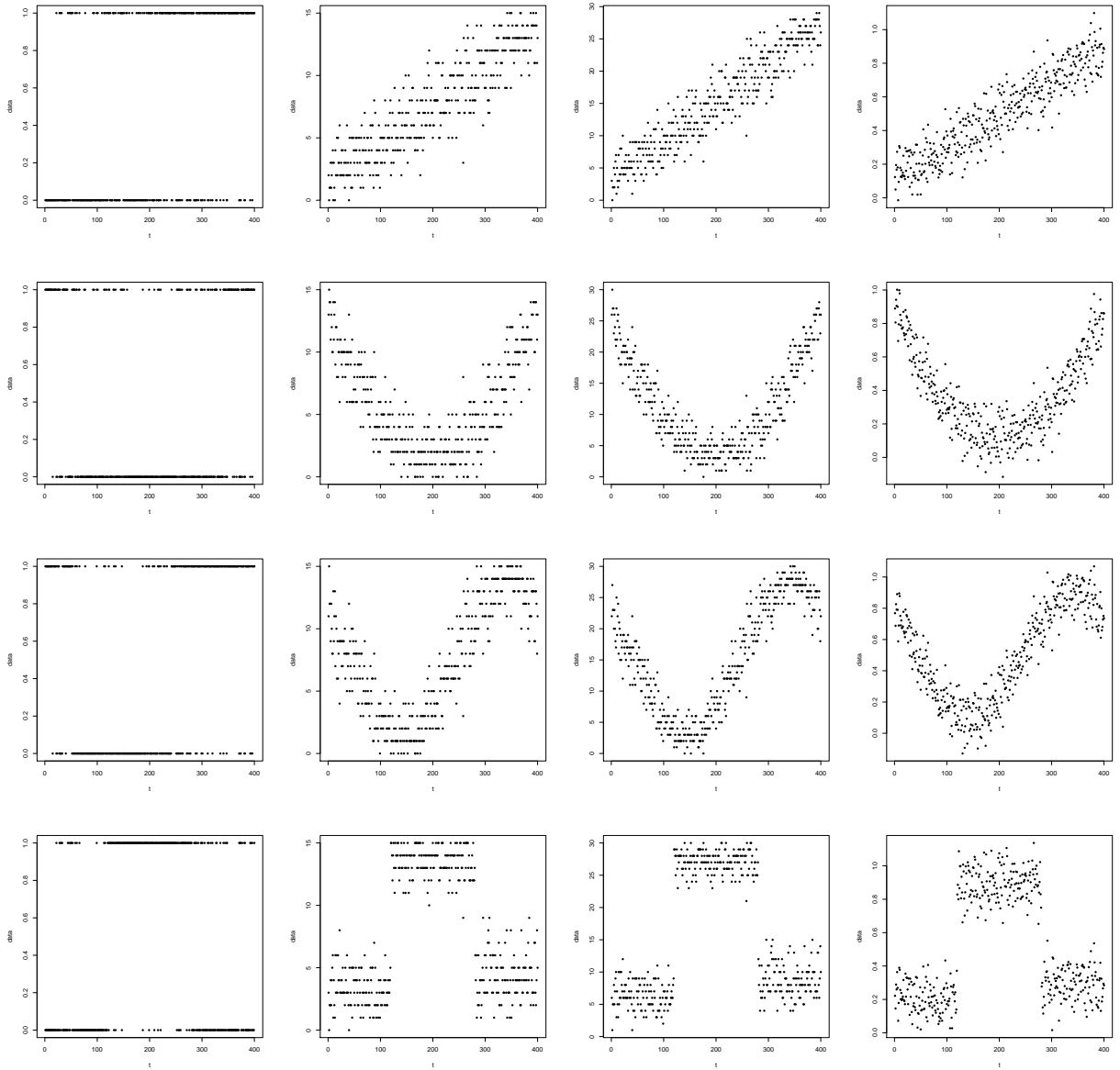


Figure 1: Data sets generated based on $\text{Bernoulli}(\alpha_t)$ (first column), $\text{bin}(15, \alpha_t)$ (second column), $\text{bin}(30, \alpha_t)$ (third column) and $N(\alpha_t, 0.1^2)$ (fourth column), considering $\alpha_t^{(k)}$ (k -th row), $k = 1, 2, 3, 4$.

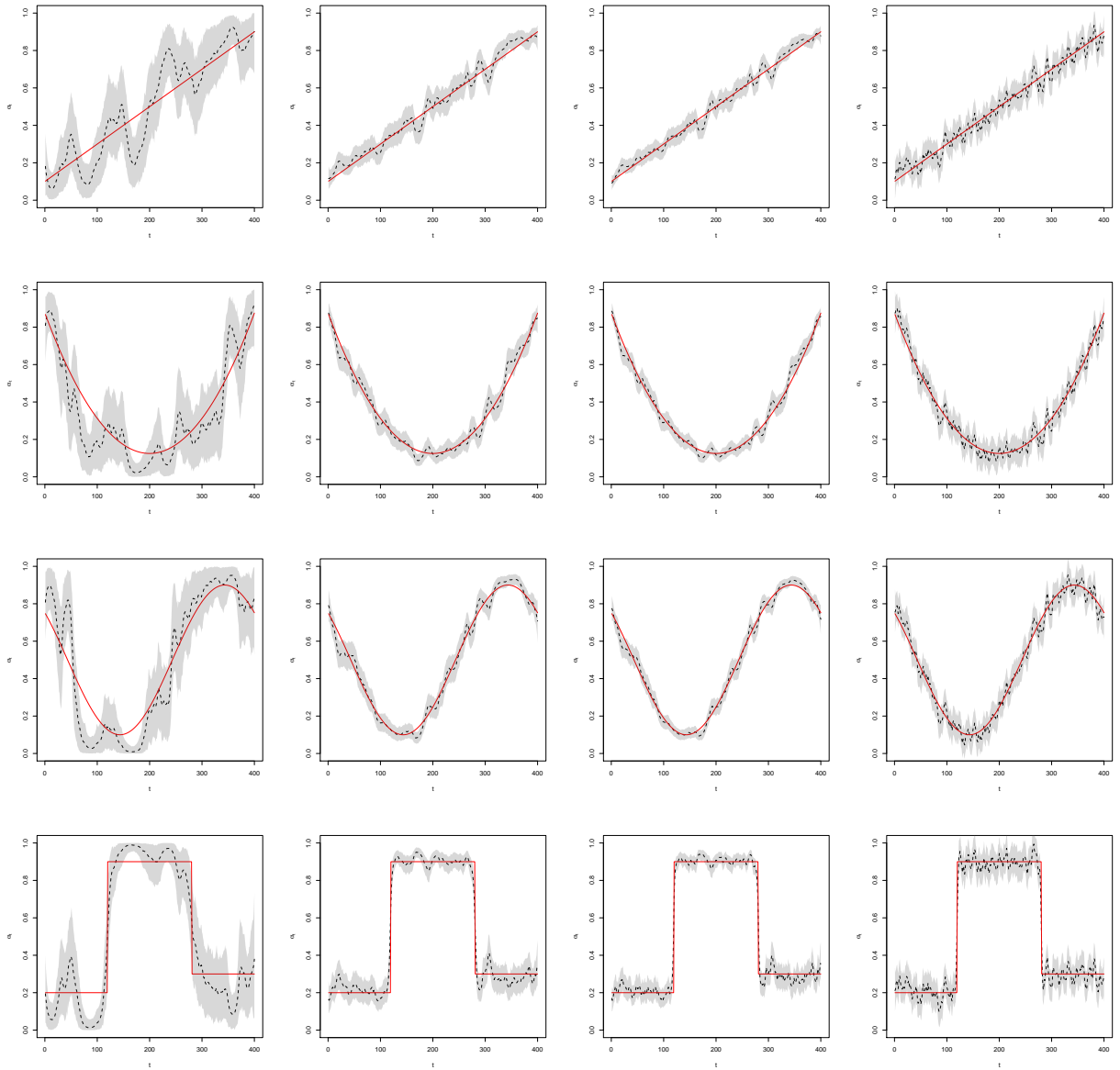


Figure 2: Estimates (dashed lines) of the α_t 's (full lines) based on the data sets $\text{Bernoulli}(\alpha_t)$ (first column), $\text{bin}(15, \alpha_t)$ (second column), $\text{bin}(30, \alpha_t)$ (third column) and $N(\alpha_t, 0.1^2)$ (fourth column), where $t = 1, 2, \dots, 400$, considering $\alpha_t^{(k)}$ (k -th row), $k = 1, 2, 3, 4$. The shaded area corresponds to the 90% HPD intervals.

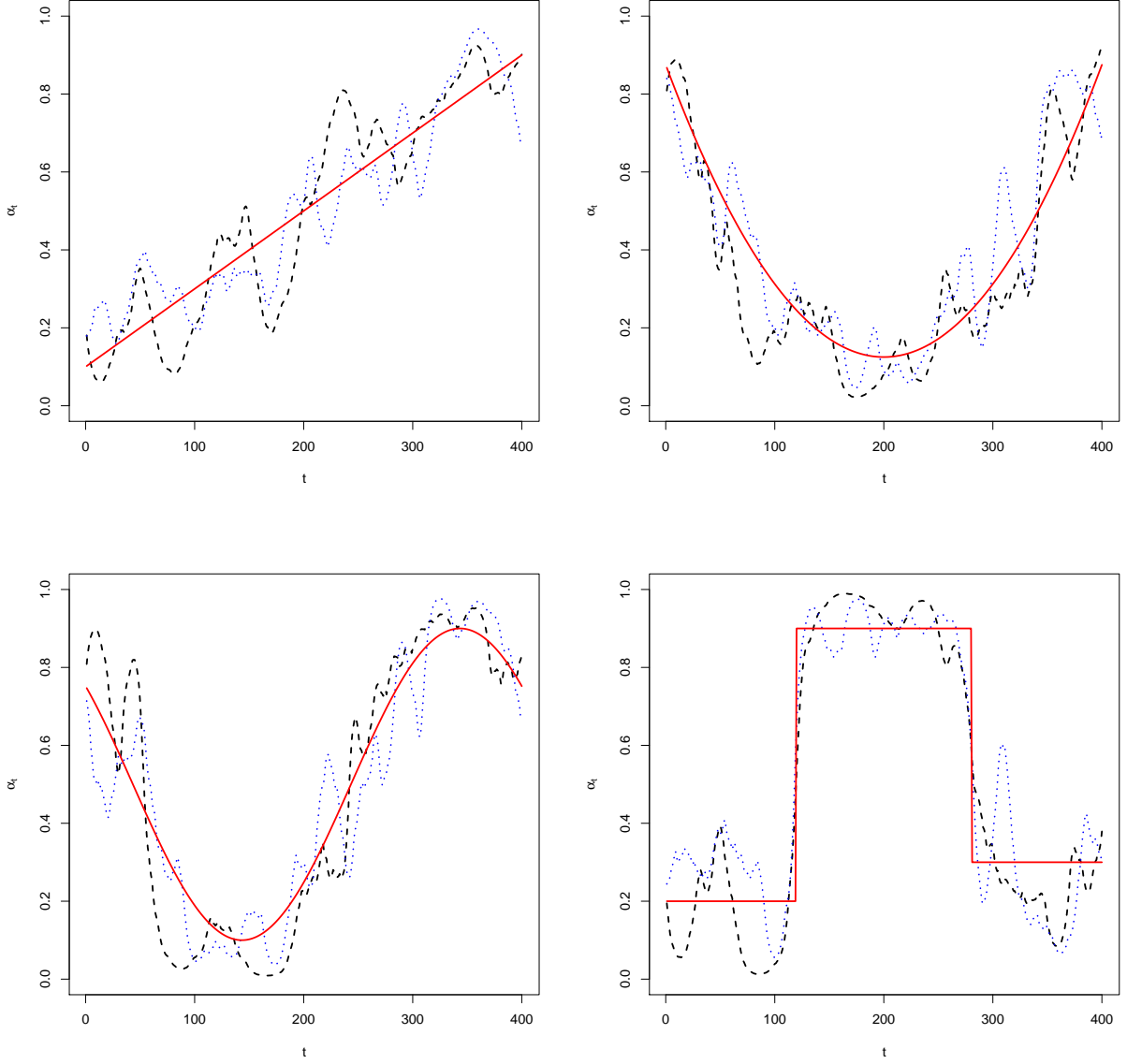


Figure 3: Comparisons of the estimates of the α_t 's (full lines) based on the logit (dashed lines) and the probit functions (dotted lines) for the data sets generated by $\text{Bernoulli}(\alpha_t)$. We consider the cases where the α_t 's have the linear behavior (top left), parabolic behavior (top right), sinusoidal behavior (bottom left) and steps behavior (bottom right). Data sets with sample size $T = 400$.

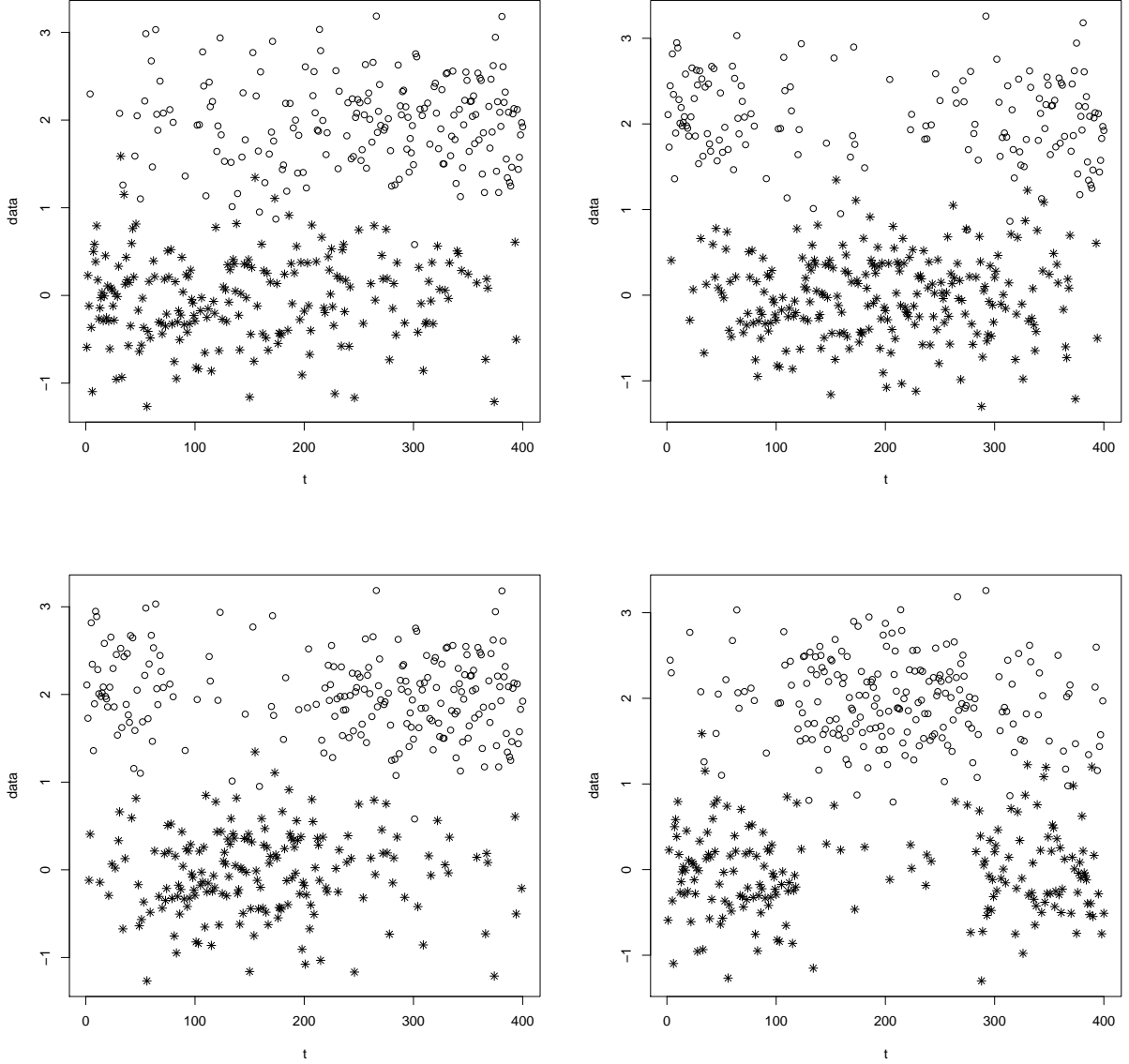


Figure 4: Data sets of size $T = 400$ generated based on the Gaussian mixture, by considering mixture weights with linear behavior (top left), parabolic behavior (top right), sinusoidal behavior (bottom left) and steps behavior (bottom right). The symbol $*$ represents $y_t \stackrel{d}{=} x_{1t}$ and o means $y_t \stackrel{d}{=} x_{2t}$.

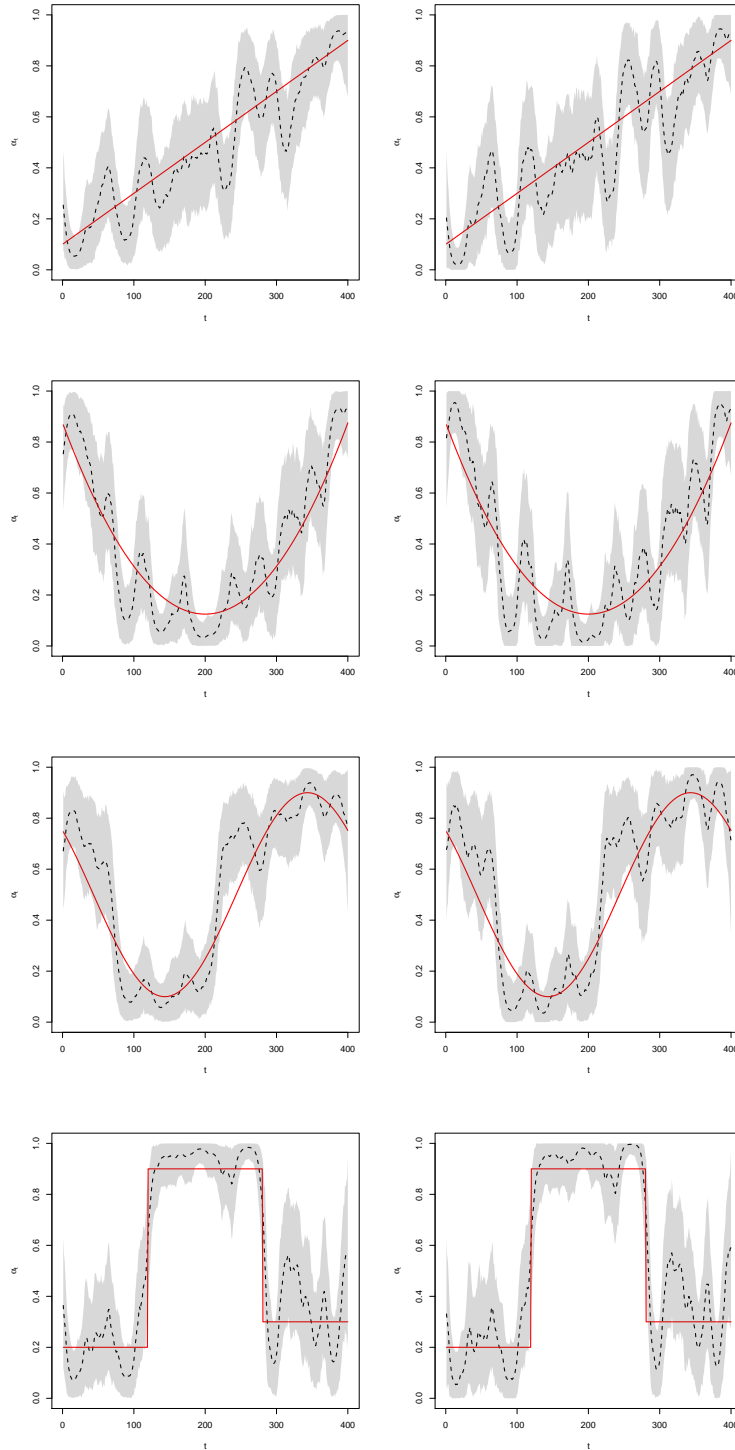


Figure 5: Estimates (dashed lines) of the α_t 's (full lines) based on the mixture data sets. The mixture weights are $\alpha_t^{(k)}$ (k -th row), $k = 1, 2, 3, 4$. The first and second columns represent estimates based on the logit and probit transforms, respectively. The shaded area corresponds to the 90% HPD intervals.

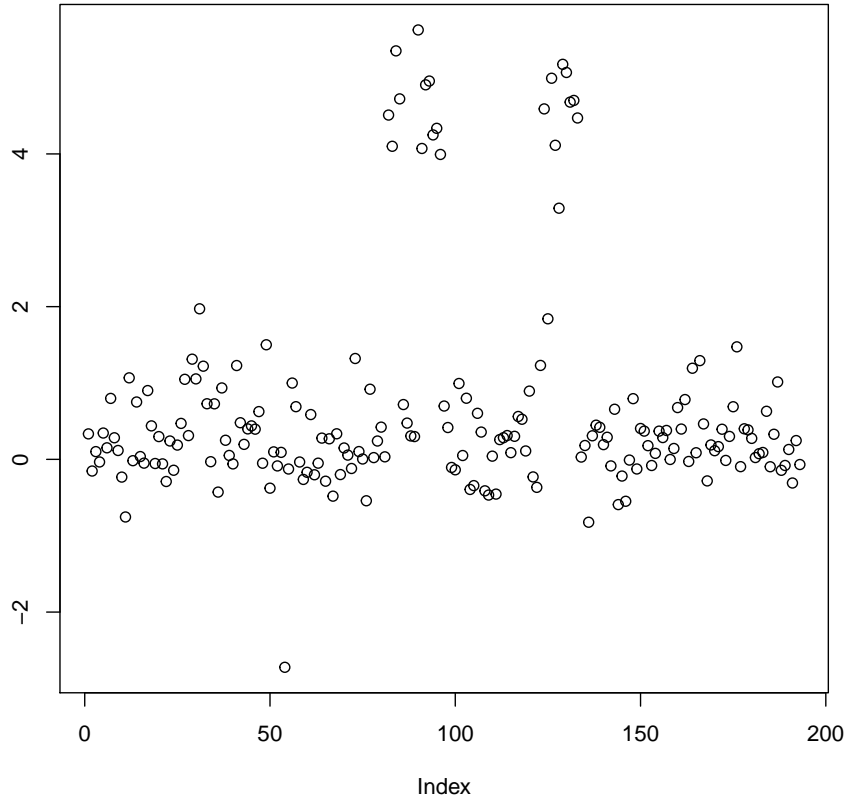


Figure 6: Observed array Comparative Genomic Hybridization (aCGH) values for $n = 193$ sampled patients. The values are log-ratios of normalized intensities from disease vs control samples, indexed by the physical location of the probes on the genome (Lai et al., 2005).

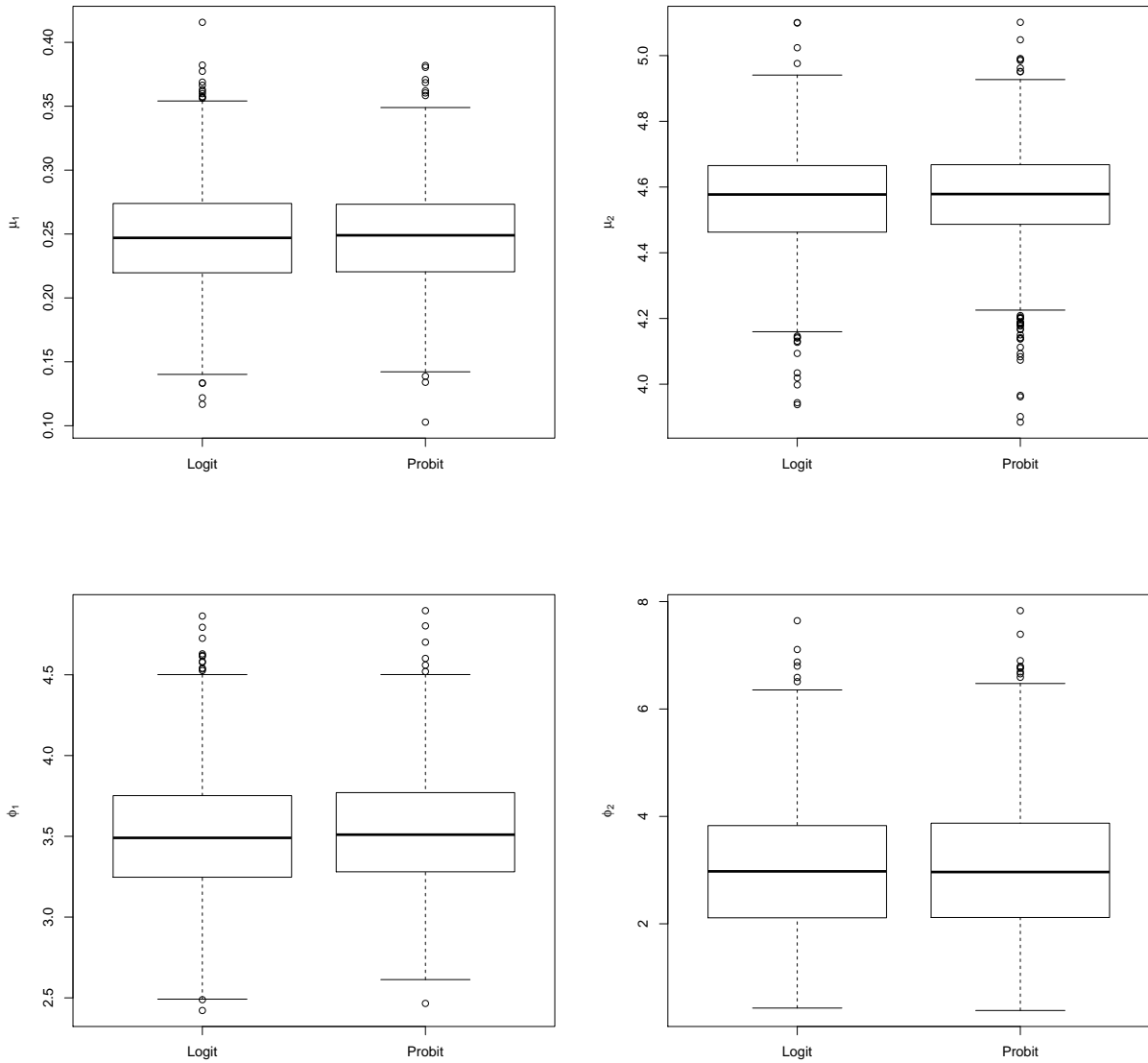


Figure 7: Boxplots of the posterior of the component parameters generated via MCMC. Each graph presents the results based on the logit and probit transforms. The first and second rows represent means (μ_1 and μ_2) and precisions (ϕ_1 and ϕ_2), respectively.

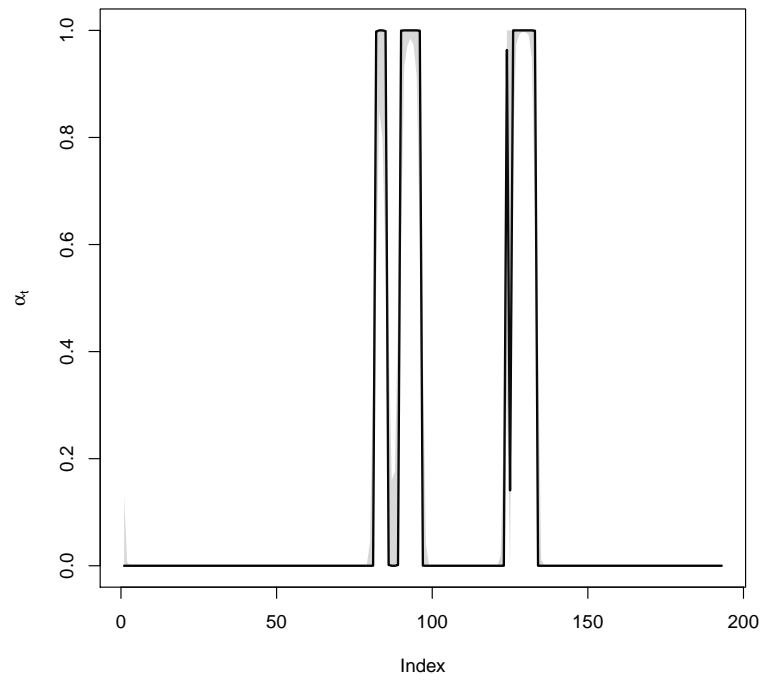
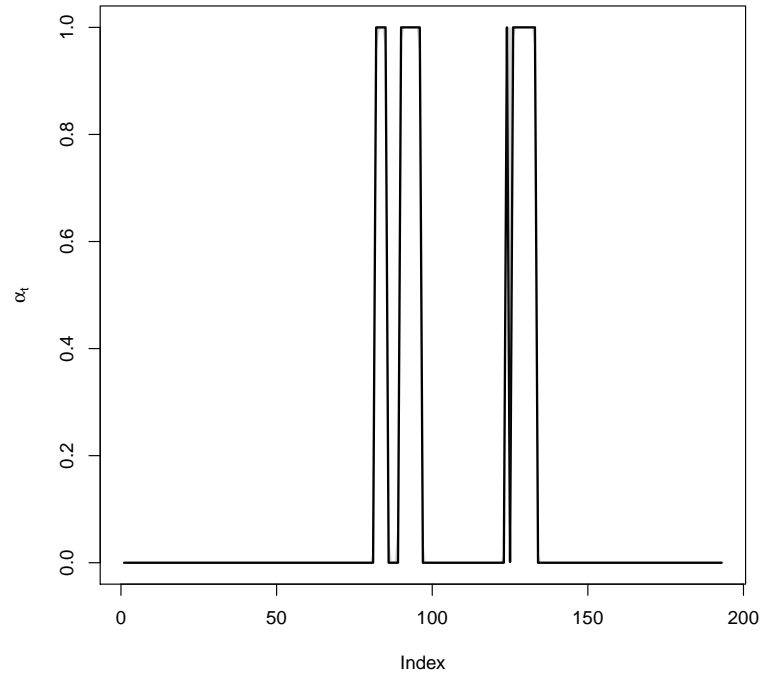


Figure 8: Estimates (full lines) of the α_t 's the aCGH data. The top and bottom pictures represent estimates based on the logit and probit link functions, respectively. The shaded area corresponds to the 90% HPD interval.

Table 1: Estimates (medians and 90% HPD credible intervals) for the component parameters $\mu_1 = 0$, $\phi_1 = 4$, $\mu_2 = 2$, $\phi_2 = 4$ of the mixture data sets generated according to each dynamical behavior: linear, parabolic, sinusoidal and steps. Both link functions, logit and probit, are considered.

Dynamical Weight	Link	$\mu_1 = 0$				$\phi_1 = 4$				$\mu_2 = 2$				$\phi_2 = 4$			
		Point Estimate	90% HPD Lower	90% HPD Upper	Point Estimate	90% HPD Lower	90% HPD Upper	Point Estimate	90% HPD Lower	90% HPD Upper	Point Estimate	90% HPD Lower	90% HPD Upper	Point Estimate	90% HPD Lower	90% HPD Upper	
Linear	Logit	-0.030	-0.091	0.038	4.081	3.274	4.979	1.965	1.900	2.039	4.093	3.184	4.905				
	Probit	-0.028	-0.102	0.037	4.041	3.231	4.919	1.968	1.899	2.042	4.081	3.153	4.970				
Parabolic	Logit	-0.018	-0.071	0.034	4.245	3.546	4.958	2.059	1.997	2.130	4.380	3.418	5.511				
	Probit	-0.018	-0.081	0.032	4.210	3.555	4.983	2.061	1.986	2.125	4.363	3.388	5.414				
Sinusoidal	Logit	-0.022	-0.086	0.041	4.140	3.343	5.039	2.008	1.956	2.065	4.765	3.943	5.679				
	Probit	-0.023	-0.092	0.035	4.138	3.403	4.972	2.007	1.952	2.061	4.758	3.928	5.631				
Steps	Logit	-0.072	-0.143	-0.004	4.499	3.516	5.631	1.924	1.851	1.992	3.557	2.843	4.284				
	Probit	-0.071	-0.140	-0.002	4.476	3.607	5.631	1.922	1.858	2.002	3.543	2.850	4.294				

Table 2: Estimates (medians and 90% HPD credible intervals) of the component parameters μ_1 , ϕ_1 , μ_2 , ϕ_2 for the aCGH data. Both link functions, logit and probit, are considered.

Mixture Parameter	Logit			Probit		
	Point Estimate	90% HPD CI		Point Estimate	90% HPD CI	
		Lower	Upper		Lower	Upper
μ_1	0.247	0.176	0.306	0.249	0.178	0.303
ϕ_1	3.491	2.903	4.143	3.510	2.929	4.180
μ_2	4.577	4.331	4.834	4.579	4.332	4.812
ϕ_2	2.977	1.046	4.773	2.965	0.992	4.894

Supplementary Material of Dynamic Weights in Gaussian Mixture Models: A Bayesian Approach

Michel H. Montoril*

Department of Statistics, Federal University of São Carlos, Brazil

and

Leandro T. Correia

Department of Statistics, University of Brasília, Brazil

and

Hélio S. Migon

Federal University of Rio de Janeiro, Brazil

*corresponding author: michel@ufscar.br

In this material we present a few proofs and derivations of results discussed in the paper. For the sake of clarity, we present the probability density function of normal and gamma r.v.'s in Section A. The proofs are available in Section B

A Main probability density functions

A.1 Normal distribution

Definition 1 We say that the random vector $\mathbf{X} = (X_1, \dots, X_p)'$ has a normal distribution with mean $\boldsymbol{\mu}$ and covariance matrix Σ , i.e., $\mathbf{X} \sim N(\boldsymbol{\mu}, \Sigma)$, if its probability density function (pdf) can be written as

$$p(\mathbf{x}|\boldsymbol{\mu}, \Sigma) = \frac{1}{\sqrt{(2\pi)^p |\Sigma|}} \exp \left\{ -\frac{1}{2} (\mathbf{x} - \boldsymbol{\mu})' \Sigma^{-1} (\mathbf{x} - \boldsymbol{\mu}) \right\}, \quad \mathbf{x} \in \mathbb{R}^p.$$

The pdf above can be represented by its kernel, which corresponds to

$$p(\mathbf{x}|\boldsymbol{\mu}, \Sigma) \propto \exp \left\{ -\frac{1}{2} \mathbf{x}' \Sigma^{-1} \mathbf{x} + \boldsymbol{\mu}' \Sigma^{-1} \mathbf{x} \right\}, \quad \mathbf{x} \in \mathbb{R}^p. \quad (\text{A.1})$$

A usual and particular case corresponds to the situation where $p = 1$, that is, \mathbf{X} is a random variable, and denoted by X . In this case we have

$$p(x|\mu, \sigma^2) = \frac{1}{\sqrt{2\pi\sigma^2}} \exp \left\{ -\frac{1}{2\sigma^2} (x - \mu)^2 \right\}, \quad x \in \mathbb{R}.$$

The kernel of the pdf above is

$$p(x|\mu, \sigma^2) \propto \exp \left\{ -\frac{1}{2\sigma^2} x^2 + \frac{\mu}{\sigma^2} x \right\}, \quad x \in \mathbb{R}. \quad (\text{A.2})$$

A.2 Gamma distribution

Definition 2 We say that the random variable X has a gamma distribution with shape and rate parameters ν and η , respectively, both positive, if its pdf is

$$p(x|\nu, \eta) = \frac{\eta^\nu}{\Gamma(\nu)} x^{\nu-1} \exp\{-\eta x\}, \quad x > 0.$$

One can write $X \sim \Gamma(\nu, \eta)$.

The kernel of the pdf above can be represented by

$$p(x|\nu, \eta) \propto x^{\nu-1} \exp\{-\eta x\}, \quad x > 0. \tag{A.3}$$

B Proofs of some results presented in the manuscript

B.1 Modifying the precision-based algorithm in the polynomial case

In this subsection, we intend to give more details about the main results presented in Section 3.2.1 (all the results before in the same section can be seen in more details in Chan and Strachan (2012)).

B.1.1 Proof of Proposition 1

In the manuscript we deal with a p -th order polynomial DLM that can be written as

$$y_t = \theta_{t1} + \epsilon_t, \tag{B.4}$$

$$\theta_{tk} = \begin{cases} \theta_{(t-1)k} + \theta_{(t-1)(k+1)} + \omega_{tk}, & k = 1, \dots, p-1, \\ \theta_{(t-1)p} + \omega_{tp}, & k = p, \end{cases} \tag{B.5}$$

where $\epsilon_t \sim N(0, V)$ and $\omega_{tk} \sim N(0, W_k)$, $k = 1, \dots, p$, $t = 1, \dots, T$, under the assumption that the innovations are independent. The model above makes clear the Markovian property (8) in the paper. Also, borrowing the matrix/vector notation used in the paper, it is easy to see that (B.4)-(B.5) can be written as

$$\mathbf{y} = \boldsymbol{\vartheta}_1 + \boldsymbol{\epsilon} \quad (\text{B.6})$$

$$\mathbf{H}\boldsymbol{\vartheta}_k = \begin{cases} (\theta_{0k} + \theta_{0(k+1)})\mathbf{e}_1 + \mathbf{B}\boldsymbol{\vartheta}_{k+1} + \boldsymbol{\omega}_k, & k = 1, \dots, p-1, \\ \theta_{0p}\mathbf{e}_1 + \boldsymbol{\omega}_p, & k = p, \end{cases} \quad (\text{B.7})$$

where \mathbf{H} , the same in Proposition 1, can be written as

$$\mathbf{H} = \begin{pmatrix} 1 & 0 & 0 & \dots & 0 & 0 \\ -1 & 1 & 0 & \dots & 0 & 0 \\ 0 & -1 & 1 & \dots & 0 & 0 \\ \vdots & \vdots & \vdots & \ddots & \vdots & \vdots \\ 0 & 0 & 0 & \dots & -1 & 1 \end{pmatrix}, \quad (\text{B.8})$$

$\mathbf{e}_1 = (1, 0, \dots, 0)'$ and $\mathbf{B} = \mathbf{I} - \mathbf{H}$. After pre-multiplying both sides by \mathbf{H}^{-1} , one can see that

$$\boldsymbol{\vartheta}_k = \boldsymbol{\mu}_k + \mathbf{H}^{-1}\boldsymbol{\omega}_k, \quad (\text{B.9})$$

where $\boldsymbol{\mu}_k = (\theta_{0k} + \theta_{0(k+1)})\mathbf{1} + (\mathbf{H}^{-1} - \mathbf{I})\boldsymbol{\vartheta}_{k+1}$, if $k = 1, \dots, p-1$, and $\boldsymbol{\mu}_p = \theta_{0p}\mathbf{1}$. Therefore, (B.6) and (B.9) yields the desired result in Proposition 1.

B.1.2 Full conditional posterior of $\boldsymbol{\vartheta}_k$ in (12)

We derive the posterior for the case where $k = 2, \dots, p-1$. For the case where $k = 1$ and $k = p$, the result is obtained similarly. In order to simplify the notation, let us denote $\Phi_k = W_k^{-1}\mathbf{H}'\mathbf{H}$ and $\mathbf{A} = (\mathbf{H}^{-1} - \mathbf{I})$. Therefore, because of Proposition 1, the posterior

of the vector $\boldsymbol{\vartheta}_k$ is determined by

$$\begin{aligned}
p(\boldsymbol{\vartheta}_k | [\dots]) &\propto p(\boldsymbol{\vartheta}_k | \boldsymbol{\vartheta}_{k+1}) p(\boldsymbol{\vartheta}_{k-1} | \boldsymbol{\vartheta}_k) \\
&\propto \exp \left\{ -\frac{1}{2} (\boldsymbol{\vartheta}_k - \boldsymbol{\mu}_k)' \boldsymbol{\Phi}_k (\boldsymbol{\vartheta}_k - \boldsymbol{\mu}_k) \right\} \\
&\quad \times \exp \left\{ -\frac{1}{2} (\boldsymbol{\vartheta}_{k-1} - \boldsymbol{\mu}_{k-1})' \boldsymbol{\Phi}_{k-1} (\boldsymbol{\vartheta}_{k-1} - \boldsymbol{\mu}_{k-1}) \right\} \\
&\propto \exp \left\{ -\frac{1}{2} (\boldsymbol{\vartheta}_k - \boldsymbol{\mu}_k)' \boldsymbol{\Phi}_k (\boldsymbol{\vartheta}_k - \boldsymbol{\mu}_k) \right\} \\
&\quad \times \exp \left\{ -\frac{1}{2} [\boldsymbol{\vartheta}_{k-1} - (\theta_{0(k-1)} + \theta_{0k}) \mathbf{1} - \mathbf{A} \boldsymbol{\vartheta}_k]' \boldsymbol{\Phi}_{k-1} [\boldsymbol{\vartheta}_{k-1} - (\theta_{0(k-1)} + \theta_{0k}) \mathbf{1} - \mathbf{A} \boldsymbol{\vartheta}_k] \right\} \\
&\propto \exp \left\{ -\frac{1}{2} \boldsymbol{\vartheta}'_k \boldsymbol{\Phi}_k \boldsymbol{\vartheta}_k + \boldsymbol{\mu}'_k \boldsymbol{\Phi}_k \boldsymbol{\vartheta}_k - \frac{1}{2} \boldsymbol{\vartheta}'_k \mathbf{A}' \boldsymbol{\Phi}_{k-1} \mathbf{A} \boldsymbol{\vartheta}_k \right. \\
&\quad \left. + (\boldsymbol{\vartheta}_{k-1} - (\theta_{0(k-1)} + \theta_{0k}) \mathbf{1})' \boldsymbol{\Phi}_{k-1} \mathbf{A} \boldsymbol{\vartheta}_k \right\} \\
&\propto \exp \left\{ -\frac{1}{2} \boldsymbol{\vartheta}'_k (\boldsymbol{\Phi}_k + \mathbf{A}' \boldsymbol{\Phi}_{k-1} \mathbf{A}) \boldsymbol{\vartheta}_k \right. \\
&\quad \left. + [(\boldsymbol{\vartheta}_{k-1} - (\theta_{0(k-1)} + \theta_{0k}) \mathbf{1})' \boldsymbol{\Phi}_{k-1} \mathbf{A} + \boldsymbol{\mu}'_k \boldsymbol{\Phi}_k] \boldsymbol{\vartheta}_k \right\} \\
&\propto \exp \left\{ -\frac{1}{2} \boldsymbol{\vartheta}'_k (\boldsymbol{\Phi}_k + \mathbf{A}' \boldsymbol{\Phi}_{k-1} \mathbf{A}) \boldsymbol{\vartheta}_k \right. \\
&\quad \left. + [\mathbf{A}' \boldsymbol{\Phi}_{k-1} (\boldsymbol{\vartheta}_{k-1} - (\theta_{0(k-1)} + \theta_{0k}) \mathbf{1}) + \boldsymbol{\Phi}_k \boldsymbol{\mu}_k]' \boldsymbol{\vartheta}_k \right\}.
\end{aligned}$$

If we denote $\bar{\boldsymbol{\Phi}}_k = \boldsymbol{\Phi}_k + \mathbf{A}' \boldsymbol{\Phi}_{k-1} \mathbf{A}$ and $\bar{\boldsymbol{\mu}}_k = \bar{\boldsymbol{\Phi}}_k^{-1} [\mathbf{A}' \boldsymbol{\Phi}_{k-1} (\boldsymbol{\vartheta}_{k-1} - (\theta_{0(k-1)} + \theta_{0k}) \mathbf{1}) + \boldsymbol{\Phi}_k \boldsymbol{\mu}_k]$, then

$$p(\boldsymbol{\vartheta}_k | [\dots]) \propto \exp \left\{ -\frac{1}{2} \boldsymbol{\vartheta}'_k \bar{\boldsymbol{\Phi}}_k \boldsymbol{\vartheta}_k + \bar{\boldsymbol{\mu}}'_k \bar{\boldsymbol{\Phi}}_k \boldsymbol{\vartheta}_k \right\},$$

which, by (A.1), corresponds to the kernel of a multivariate normal distribution. Hence,

$$\boldsymbol{\vartheta}_k | [\dots] \sim N(\bar{\boldsymbol{\mu}}_k, \bar{\boldsymbol{\Phi}}_k^{-1}),$$

where

$$\begin{aligned}\bar{\Phi}_k &= \mathbf{A}' \Phi_{k-1} \mathbf{A} + \Phi_k = \frac{1}{W_{k-1}} \mathbf{A}' \mathbf{H}' \mathbf{H} \mathbf{A} + \frac{1}{W_k} \mathbf{H}' \mathbf{H} \\ &= \frac{1}{W_{k-1}} \mathbf{B}' \mathbf{B} + \frac{1}{W_k} \mathbf{H}' \mathbf{H},\end{aligned}$$

with $\mathbf{H} \mathbf{A} = \mathbf{H} (\mathbf{H}^{-1} - \mathbf{I}) = (\mathbf{I} - \mathbf{H}) = \mathbf{B}$, and

$$\begin{aligned}\bar{\boldsymbol{\mu}}_k &= \bar{\Phi}_k^{-1} \left\{ \mathbf{A}' \Phi_{k-1} [\boldsymbol{\vartheta}_{k-1} - (\theta_{0(k-1)} + \theta_{0k}) \mathbf{1}] + \Phi_k \boldsymbol{\mu}_k \right\} \\ &= \bar{\Phi}_k^{-1} \left\{ \frac{1}{W_{k-1}} \mathbf{A}' \mathbf{H}' \mathbf{H} [\boldsymbol{\vartheta}_{k-1} - (\theta_{0(k-1)} + \theta_{0k}) \mathbf{1}] \right. \\ &\quad \left. + \frac{\theta_{0k} + \theta_{0(k+1)}}{W_k} \mathbf{H}' \mathbf{H} \mathbf{1} + \mathbf{H}' \mathbf{H} (\mathbf{H}^{-1} - \mathbf{I}) \boldsymbol{\vartheta}_{k+1} \right\} \\ &= \bar{\Phi}_k^{-1} \left\{ \frac{1}{W_{k-1}} \mathbf{B}' \mathbf{H} \boldsymbol{\vartheta}_{k-1} + \frac{\theta_{0k} + \theta_{0(k+1)}}{W_k} \mathbf{e}_1 + \frac{1}{W_k} \mathbf{H}' \mathbf{B} \boldsymbol{\vartheta}_{k+1} \right\}.\end{aligned}$$

In the last equality above, we used two results. The first,

$$\mathbf{H} \mathbf{1} = \begin{pmatrix} 1 & 0 & 0 & \dots & 0 & 0 \\ -1 & 1 & 0 & \dots & 0 & 0 \\ 0 & -1 & 1 & \dots & 0 & 0 \\ \vdots & \vdots & \vdots & \ddots & \vdots & \vdots \\ 0 & 0 & 0 & \dots & -1 & 1 \end{pmatrix} \begin{pmatrix} 1 \\ 1 \\ 1 \\ \vdots \\ 1 \end{pmatrix} = \begin{pmatrix} 1 \\ 0 \\ 0 \\ \vdots \\ 0 \end{pmatrix} = \mathbf{e}_1,$$

which provides $\mathbf{H}'\mathbf{H}\mathbf{1} = \mathbf{e}_1$. The second result is

$$\mathbf{A}'\mathbf{H}'\mathbf{H}\mathbf{1} = \mathbf{A}'\mathbf{e}_1 = \begin{pmatrix} 0 & 1 & 1 & 1 & \dots & 1 & 1 \\ 0 & 0 & 1 & 1 & \dots & 1 & 1 \\ 0 & 0 & 0 & 1 & \dots & 1 & 1 \\ \vdots & \vdots & \vdots & \vdots & \ddots & \vdots & \vdots \\ 0 & 0 & 0 & 0 & \dots & 0 & 1 \\ 0 & 0 & 0 & 0 & \dots & 0 & 0 \end{pmatrix} \begin{pmatrix} 1 \\ 0 \\ 0 \\ \vdots \\ 0 \\ 0 \end{pmatrix} = \begin{pmatrix} 0 \\ 0 \\ 0 \\ \vdots \\ 0 \\ 0 \end{pmatrix}.$$

B.1.3 Full conditional posterior of θ_{0k} in (13)

The full conditional posterior of θ_{0k} can be derived using its prior and the distribution of the terms in the model where it is associated, which are

$$\theta_{1(k-1)} = \theta_{0(k-1)} + \theta_{0k} + \omega_{1(k-1)},$$

$$\theta_{1k} = \theta_{0k} + \theta_{0(k+1)} + \omega_{1k}$$

in (B.5). Thus, we have that

$$\begin{aligned}
p(\theta_{0k} | [\dots]) &\propto p(\theta_{0k} | \mu_{\theta_{0k}}, \sigma_{\theta_{0k}}^2) p(\theta_{1(k-1)} | \theta_{0k}, \theta_{0(k-1)}, W_{k-1}) p(\theta_{1k} | \theta_{0k}, \theta_{0(k+1)}, W_k) \\
&\propto \exp \left\{ -\frac{1}{2\sigma_{\theta_{0k}}^2} (\theta_{0k} - \mu_{\theta_{0k}})^2 \right\} \exp \left\{ -\frac{1}{2W_{k-1}} (\theta_{1(k-1)} - \theta_{0(k-1)} - \theta_{0k})^2 \right\} \\
&\quad \times \exp \left\{ -\frac{1}{2W_{k-1}} (\theta_{1k} - \theta_{0k} - \theta_{0(k+1)})^2 \right\} \\
&\propto \exp \left\{ -\frac{1}{2\sigma_{\theta_{0k}}^2} \theta_{0k}^2 + \frac{\mu_{\theta_{0k}}}{\sigma_{\theta_{0k}}^2} \theta_{0k} \right\} \exp \left\{ -\frac{1}{2W_{k-1}} \theta_{0k}^2 + \frac{\theta_{1(k-1)} - \theta_{0(k-1)}}{W_{k-1}} \theta_{0k} \right\} \\
&\quad \times \exp \left\{ -\frac{1}{2W_k} \theta_{0k}^2 + \frac{\theta_{1k} - \theta_{0(k+1)}}{W_k} \theta_{0k} \right\} \\
&\propto \exp \left\{ -\frac{1}{2} \left(\frac{1}{\sigma_{\theta_{0k}}^2} + \frac{1}{W_{k-1}} + \frac{1}{W_k} \right) \theta_{0k}^2 \right. \\
&\quad \left. + \left(\frac{\mu_{\theta_{0k}}}{\sigma_{\theta_{0k}}^2} + \frac{\theta_{1(k-1)} - \theta_{0(k-1)}}{W_{k-1}} + \frac{\theta_{1k} - \theta_{0(k+1)}}{W_k} \right) \theta_{0k} \right\} \\
&\propto \exp \left\{ \frac{1}{2 \left(\frac{1}{\sigma_{\theta_{0k}}^2} + \frac{1}{W_{k-1}} + \frac{1}{W_k} \right)^{-1}} \theta_{0k}^2 \right. \\
&\quad \left. + \frac{\left(\frac{1}{\sigma_{\theta_{0k}}^2} + \frac{1}{W_{k-1}} + \frac{1}{W_k} \right)^{-1} \left(\frac{\mu_{\theta_{0k}}}{\sigma_{\theta_{0k}}^2} + \frac{\theta_{1(k-1)} - \theta_{0(k-1)}}{W_{k-1}} + \frac{\theta_{1k} - \theta_{0(k+1)}}{W_k} \right)}{\left(\frac{1}{\sigma_{\theta_{0k}}^2} + \frac{1}{W_{k-1}} + \frac{1}{W_k} \right)^{-1}} \theta_{0k} \right\}
\end{aligned}$$

Thus, based on (A.2),

$$\theta_{0k} | [\dots] \sim N(\bar{\mu}_{\theta_{0k}}, \bar{\sigma}_{\theta_{0k}}^2),$$

where

$$\begin{aligned}
\bar{\sigma}_{\theta_{0k}}^2 &= \left(\frac{1}{\sigma_{\theta_{0k}}^2} + \frac{1}{W_{k-1}} + \frac{1}{W_k} \right)^{-1}, \\
\bar{\mu}_{\theta_{0k}} &= \bar{\sigma}_{\theta_{0k}}^2 \left(\frac{\mu_{\theta_{0k}}}{\sigma_{\theta_{0k}}^2} + \frac{\theta_{1(k-1)} - \theta_{0(k-1)}}{W_{k-1}} + \frac{\theta_{1k} - \theta_{0(k+1)}}{W_k} \right).
\end{aligned}$$

B.1.4 Full conditional posterior of W_k^{-1} in (14) and V^{-1} in (15)

The posterior distribution of the precision W_k^{-1} involves its prior distribution and the distribution of $\boldsymbol{\vartheta}_k | \boldsymbol{\vartheta}_{k+1}$ in Proposition 1. Assuming that $W_k^{-1} \sim \Gamma(\nu_{0k}, \eta_{0k})$, we have

$$\begin{aligned} p(W_k^{-1}) &\propto p(W_k^{-1} | \nu_{0k}, \eta_{0k}) p(\boldsymbol{\vartheta}_k | \boldsymbol{\vartheta}_{k+1}) \\ &\propto \frac{1}{W_k^{\nu_{0k}-1}} \exp\left\{-\frac{\eta_{0k}}{W_k}\right\} \frac{1}{W_k^{T/2}} \exp\left\{-\frac{1}{2W_k}(\boldsymbol{\vartheta}_k - \boldsymbol{\mu}_k)' \mathbf{H}' \mathbf{H}(\boldsymbol{\vartheta}_k - \boldsymbol{\mu}_k)\right\} \\ &\propto (W_k^{-1})^{\nu_{0k} + \frac{T}{2} - 1} \exp\left\{-\left[\eta_{0k} + \frac{1}{2}(\boldsymbol{\vartheta}_k - \boldsymbol{\mu}_k)' \mathbf{H}' \mathbf{H}(\boldsymbol{\vartheta}_k - \boldsymbol{\mu}_k)\right] W_k^{-1}\right\}, \end{aligned}$$

which, by (A.3), ensures that

$$W_k^{-1} | [\dots] \sim \Gamma(\bar{\nu}_{0k}, \bar{\eta}_{0k}),$$

where

$$\begin{aligned} \bar{\nu}_{0k} &= \nu_{0k} + \frac{T}{2}, \\ \bar{\eta}_{0k} &= \eta_{0k} + \frac{1}{2}(\boldsymbol{\vartheta}_k - \boldsymbol{\mu}_k)' \mathbf{H}' \mathbf{H}(\boldsymbol{\vartheta}_k - \boldsymbol{\mu}_k), \end{aligned}$$

The full conditional posterior of V^{-1} can be derived analogously.

B.2 Proof of Theorem 1

In order to prove this theorem, we make use of the following lemma (a sketch of its proof is provided at the end).

Lemma 1 *Let $\boldsymbol{\beta}_{(k)} = (\beta_1, \beta_2, \dots, \beta_{k-1}, \beta_{k+1}, \dots, \beta_n)'$. If $\boldsymbol{\beta} \sim N(\boldsymbol{\mu}, W(\mathbf{H}' \mathbf{H})^{-1})$, with \mathbf{H} defined as in (B.8). Then,*

$$\beta_k | \boldsymbol{\beta}_{(k)} \sim N(\tilde{\mu}_k, \tilde{\sigma}_k^2),$$

where

$$\tilde{\mu}_k = \begin{cases} \mu_1 + \frac{1}{2}(\beta_2 - \mu_2), & \text{if } k = 1, \\ \mu_k + \frac{1}{2}[(\beta_{k-1} + \beta_{k+1}) - (\mu_{k-1} + \mu_{k+1})], & \text{if } k = 2, \dots, n-1, \\ \mu_n + (\beta_{n-1} - \mu_{n-1}), & \text{if } k = n, \end{cases}$$

and

$$\tilde{\sigma}_k^2 = \begin{cases} \frac{\omega_1^2}{2}, & \text{if } k = 2, \dots, n-1, \\ \omega_1^2, & \text{if } k = n. \end{cases}$$

Going back to the proof of Theorem 1, by (10) in Proposition 1,

$$\boldsymbol{\vartheta}_1 | \boldsymbol{\vartheta}_2 \sim N \left[\boldsymbol{\mu}_1, W_1 \left(\mathbf{H}' \mathbf{H} \right)^{-1} \right],$$

where $\boldsymbol{\mu}_1 = (\theta_{01} + \theta_{02})\mathbf{1} + (\mathbf{H}^{-1} - \mathbf{I})\boldsymbol{\vartheta}_2$. Then, by Lemma 1,

$$\theta_{t1} | \boldsymbol{\vartheta}_{(t)1}, \boldsymbol{\vartheta}_2 \sim N(\mu_{t1}^*, \tau_t^2),$$

where

$$\tau_t^2 = \begin{cases} \frac{W_1}{2}, & \text{if } t = 1, \dots, T-1, \\ W_1, & \text{if } t = T. \end{cases} \quad (\text{B.10})$$

With respect to the mean, one can see that

$$\mathbf{H}^{-1} - \mathbf{I} = \begin{pmatrix} 0 & 1 & 1 & 1 & \dots & 1 & 1 \\ 0 & 0 & 1 & 1 & \dots & 1 & 1 \\ 0 & 0 & 0 & 1 & \dots & 1 & 1 \\ \vdots & \vdots & \vdots & \vdots & \ddots & \vdots & \vdots \\ 0 & 0 & 0 & 0 & \dots & 0 & 1 \\ 0 & 0 & 0 & 0 & \dots & 0 & 0 \end{pmatrix}.$$

Thus, each element of $\boldsymbol{\mu}_1$ can be written as

$$\mu_{t1} = \sum_{t=0}^{t-1} \theta_{t2} + \theta_{01} = \mu_{(t-1)1} + \theta_{(t-1)2}, \quad (\text{B.11})$$

$t = 1, \dots, T$. Hence, based on (B.11), we have the following results. For $t = 1$,

$$\begin{aligned} \mu_{11}^* &= \mu_{11} + \frac{1}{2}(\theta_{21} - \mu_{12}) \\ &= \mu_{11} - \frac{1}{2}\mu_{21} + \frac{1}{2}\theta_{21} \\ &= \mu_{11} - \frac{1}{2}(\mu_{11} + \theta_{12}) + \frac{1}{2}\theta_{21} \\ &= \frac{1}{2}\mu_{11} + \frac{1}{2}(\theta_{21} - \theta_{12}) \\ &= \frac{1}{2}(\theta_{01} + \theta_{02}) + \frac{1}{2}(\theta_{21} - \theta_{12}). \end{aligned} \quad (\text{B.12})$$

For $t = 2, \dots, T - 1$,

$$\begin{aligned} \mu_{t1}^* &= \mu_{t1} + \frac{1}{2} [(\theta_{(t-1)1} + \theta_{(t+1)1}) - (\mu_{(t-1)1} + \mu_{(t+1)1})] \\ &= \frac{1}{2} [(\theta_{(t-1)1} + \theta_{(t+1)1}) + (\mu_{t1} - \mu_{(t-1)1}) - (\mu_{(t+1)1} - \mu_{t1})] \\ &= \frac{1}{2} (\theta_{(t-1)1} + \theta_{(t+1)1} + \theta_{(t-1)2} - \theta_{t2}) \\ &= \frac{1}{2} (\theta_{(t+1)1} - \theta_{t2}) + \frac{1}{2} (\theta_{(t-1)1} + \theta_{(t-1)2}). \end{aligned} \quad (\text{B.13})$$

Finally,

$$\begin{aligned} \mu_{T1}^* &= \mu_{T1} + (\theta_{(T-1)1} - \mu_{(T-1)1}) \\ &= \theta_{(T-1)2} + \theta_{(T-1)1} \end{aligned} \quad (\text{B.14})$$

The desired result follows from (B.10), (B.12)–(B.14).

Proof of Lemma 1. The algebra to prove this result is extremely tedious. Thus, for the

sake of simplicity, let us consider the particular case where $n = 5$. We have that

$$\mathbf{H}'\mathbf{H} = \begin{pmatrix} 2 & -1 & 0 & 0 & 0 \\ -1 & 2 & -1 & 0 & 0 \\ 0 & -1 & 2 & -1 & 0 \\ 0 & 0 & -1 & 2 & -1 \\ 0 & 0 & 0 & -1 & 1 \end{pmatrix} \quad \text{and} \quad (\mathbf{H}'\mathbf{H})^{-1} = \begin{pmatrix} 1 & 1 & 1 & 1 & 1 \\ 1 & 2 & 2 & 2 & 2 \\ 1 & 2 & 3 & 3 & 3 \\ 1 & 2 & 3 & 4 & 4 \\ 1 & 2 & 3 & 4 & 5 \end{pmatrix}$$

Let us consider $k = 1$. In this case, $\boldsymbol{\beta}$ is partitioned in $\boldsymbol{\beta}_1 = \beta_1$ and $\boldsymbol{\beta}_2 = (\beta_2, \beta_3, \beta_4, \beta_5)'$.

Denoting $\boldsymbol{\mu}_1 = \mu_1$, $\boldsymbol{\mu}_2 = (\mu_2, \mu_3, \mu_4, \mu_5)'$, and $\boldsymbol{\Sigma}_{11} = W$, $\boldsymbol{\Sigma}_{12} = W(1, 1, 1, 1)' = \boldsymbol{\Sigma}'_{21}$,

$$\boldsymbol{\Sigma}_{22} = W \begin{pmatrix} 2 & 2 & 2 & 2 \\ 2 & 3 & 3 & 3 \\ 2 & 3 & 4 & 4 \\ 2 & 3 & 4 & 5 \end{pmatrix},$$

we can apply the well-known result to derive the conditional distribution of partitions of a multivariate normal vector. In other words, we have that

$$\beta_1 | \boldsymbol{\beta}_{(1)} \sim N(\tilde{\mu}, \tilde{\sigma}^2),$$

where $\tilde{\sigma}^2 = \boldsymbol{\Sigma}_{11} - \boldsymbol{\Sigma}_{12}\boldsymbol{\Sigma}_{22}^{-1}\boldsymbol{\Sigma}_{21} = \frac{W}{2}$ and

$$\tilde{\mu} = \boldsymbol{\mu}_1 - \boldsymbol{\Sigma}_{12}\boldsymbol{\Sigma}_{22}^{-1}(\boldsymbol{\beta}_2 - \boldsymbol{\mu}_2) = \mu_1 - (0.5, 0, 0, 0)(\boldsymbol{\beta}_2 - \boldsymbol{\mu}_2) = \mu_1 - \frac{1}{2}(\beta_2 - \mu_2).$$

The remaining results for $k = 2, 3, 4, 5$ are derived analogously. ■

B.3 Full conditional posterior of $\boldsymbol{\vartheta}_1$ in (16)

In this case we have $y_t|\alpha_t \sim \text{Bern}(\alpha_t)$, with $\alpha_t = \Phi(\theta_{t1})$ and θ_{t1} representing the local level of the state equation, $t = 1, \dots, T$. Basically, one can write $\alpha_t = P(y_t = 1) = \Phi(\theta_{t1}) \equiv \Phi(\mathbf{e}'_t \boldsymbol{\vartheta}_1)$, where \mathbf{e}_t corresponds to the t -th column of an identity matrix of order T . This identity matrix plays the role of the design matrix in the probit model. Therefore, the desired result comes from the data augmentation method proposed by Albert and Chib (1993). In the present case $\boldsymbol{\vartheta}_1$ has, by Proposition 1, the prior

$$\boldsymbol{\vartheta}_1|\boldsymbol{\vartheta}_2 \sim N\left(\boldsymbol{\mu}_1, W_1(\mathbf{H}'\mathbf{H})\right),$$

with $\boldsymbol{\mu}_1 = (\theta_{01} + \theta_{02})\mathbf{1} + (\mathbf{H}^{-1} - \mathbf{I})\boldsymbol{\vartheta}_2$.

References

- Albert, J. H. and Chib, S. (1993). Bayesian Analysis of Binary and Polychotomous Response Data. *Journal of the American Statistical Association*, 88(422):669–679.
- Chan, J. C. C. and Strachan, R. W. (2012). Estimation in Non-Linear Non-Gaussian State Space Models with Precision-Based Methods. CAMA Working Papers 2012-13, Centre for Applied Macroeconomic Analysis, Crawford School of Public Policy, The Australian National University.